Taylor & Francis
Taylor & Francis Group

Check for updates

Molecular basis for the repurposing of histamine H2-receptor antagonist to treat COVID-19

Ahmed A. Ishola[a], Tanuja Joshi[b,c], Suliat I. Abdulai[d], Habibu Tijjani[e] (iD), Hemlata Pundir[b] and Subhash Chandra[b,c] (iD)

[a]Department of Biochemistry, Faculty of Life Sciences, University of Ilorin, Ilorin, Nigeria; [b]Computational Biology & Biotechnology Laboratory, Department of Botany, Soban Singh Jeena University, Almora, Uttarakhand, India; [c]Department of Botany, Kumaun University, S.S.J Campus, Almora, Uttarakhand, India; [d]Central Research Laboratory, Ilorin, Kwara State, Nigeria; [e]Department of Biochemistry, Natural Product Research Laboratory, Bauchi State University, Gadau, Nigeria

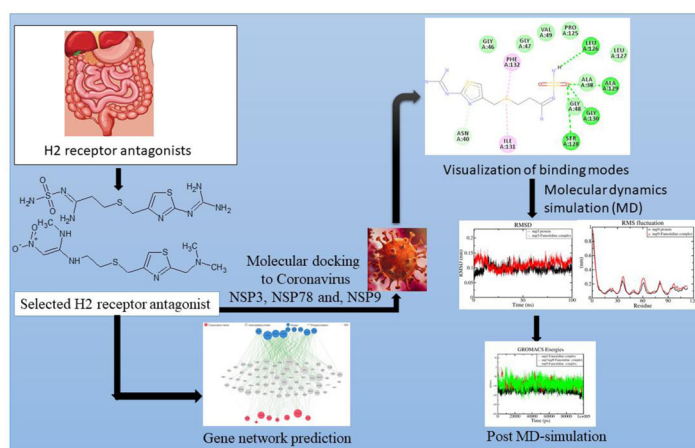Communicated by Ramaswamy H. Sarma

ABSTRACT

With the world threatened by a second surge in the number of Coronavirus cases, there is an urgent need for the development of effective treatment for the novel coronavirus (COVID-19). Recently, global attention has turned to preliminary reports on the promising anti-COVID-19 effect of histamine H2-receptor antagonists (H2RAs), most especially Famotidine. Therefore, this study was designed to exploit a possible molecular basis for the efficacy of H2RAs against coronavirus. Molecular docking was performed between four H2RAs, Cimetidine, Famotidine, Nizatidine, Ranitidine, and three non-structural proteins viz. NSP3, NSP7/8 complex, and NSP9. Thereafter, a 100 ns molecular dynamics simulation was carried out with the most outstanding ligands to determine the stability. Thereafter, Famotidine and Cimetidine were subjected to gene target prediction analysis using HitPickV2 and eXpression2Kinases server to determine the possible network of genes associated with their anti-COVID activities. Results obtained from molecular docking showed the superiority of Famotidine and Cimetidine compared to other H2RAs with a higher binding affinity to all selected targets. Molecular dynamic simulation and MMPBSA results revealed that Famotidine as well as Cimetidine bind to non-structural proteins more efficiently with high stability over 100 ns. Results obtained suggest that Famotidine and Cimetidine could be a viable option to treat COVID-19 with a mechanism of action that involves the inhibition of viral replication through the inhibition of non-structural proteins. Therefore, Famotidineand Cimetidine qualify for further study as a potential treatment for COVID-19.

Introduction

Severe Acute Respiratory Syndrome Coronavirus-2 (SARS-CoV-2) also known as COVID-19 originated from Wuhan in China and has spread to almost all countries with severe fatalities recorded. COVID-19 continues to create havoc with over 11 million cases and 532,000 deaths globally as of 6th July 2020 (WHO, 2020). COVID-19 is believed to

CONTACT Tanuja Joshi ✉ joshitanuja222@gmail.com; Subhash Chandra ✉ scjnu@yahoo.co.in 🖳 Computational Biology & Biotechnology Laboratory, Department of Botany, Soban Singh Jeena University, Almora, Uttarakhand, India

have originated from the bat with over 90% similarity in its genomic sequence. Among all known RNA viruses, the coronavirus RNA genome (ranging from 26 to 32 kb) is the largest and the viral particle is around 125 nm in diameter (Ji et al., 2020). The genes that encodes for non-structural proteins make up two-thirds of the CoV genome. The evolution of new strains and adaptability in new hosts may be attributed to the ability of SARS-CoV-2 to recombine, leading to novel strains with diverse hosts (Ishola & Asogwa, 2020).

The SARS-CoV-2 proteins consist of two large polyproteins: ORF1a and ORF1ab (which form 16 non-structural proteins by proteolytic cleavage), four structural proteins: spike (S), envelope (E), membrane (M) and nucleocapsid (N), and eight accessory proteins like ORF3a, ORF3b, ORF6, ORF7a, ORF7b, ORF8a, ORF8b, and ORF9b (Yoshimoto, 2020).

Nonstructural Protein 3 (NSP3) (approximately 200 kD) is a multifunctional protein containing up to 16 distinct domains and regions. NSP3 binds to viral RNA, nucleocapsid protein and other viral proteins and participates in the synthesis of polyproteins (Lei et al., 2018). NSP8 is a peptide cofactor which makes a heterodimeric complex with NSP7, and this NSP7/8 heterodimer complex with NSP12. The NSP12-NSP7/8 sub-complex is therefore defined as the minimal core component mediating the RNA synthesis of coronavirus (Peng et al., 2020). Coronavirus non-structural protein 9 (NSP9) is important for replication during human cell infection.

Histamine H2-receptor antagonists (H2RAs) are mostly used in patients with acid-related disorders such as gastroesophageal reflux disease, and peptic ulcer disease (Adachi et al., 2005). H2RAs have been used in many other treatments, such as cancer, virus infection, bone remodeling, burn treatment, and vaccine enhancer, with inconsistent outcomes (Jafarzadeh et al., 2019). Some common H2RAs are Cimetidine, Famotidine, Nizatidine, and Ranitidine. Famotidine, a propanimidamide, has a competitive inhibitory function on histamine H2-receptors found on the basolateral membrane of the parietal cell. Recently, scientists are exploring possibilities of the use of Famotidine as a therapeutic agent against COVID-19. Retrospective research on Famotidine found a decreased risk of clinical decline leading to intubation or death in patients diagnosed with COVID-19 treated with the drug (Freedberg et al., 2020). Another study involving ten non-hospitalized patients associated with positive symptoms as shortness of breath and cough consistent with the use of high-dose oral Famotidine (Janowitz et al., 2020). Clinical trials are ongoing to assess the potency of a variety of drugs, however, many of these drugs are toxic and so far, no drug completely cured the disease. The Phase-III trial, 'Multi-site Adaptive Experiments of Hydroxychloroquine and Famotidine' is currently being launched.

This randomized double-blind clinical trial (N^1/41170) has been outlined to compare clinical outcomes between two arms: the first receiving hydroxychloroquine 200 mg plus Famotidine (360 mg/d intravenously) with the other arm receiving hydroxychloroquine plus placebo. However, knowledge about possible molecular targets for H2RAs among coronavirus proteins is very scanty. Therefore, we investigate the possible targets for H2RAs among selected coronavirus non-structural proteins using molecular docking and molecular dynamics simulation approach.

Materials and method

Antiviral activity prediction

Anti-viral activity and percentage inhibition of compounds against several viruses can be checked by using the AVCpred server (Qureshi et al., 2017). The AVCpred server uses a web-based algorithm based on validated experimental data to predict antiviral compounds. The server employs integrated Quantitative structure-activity relationships (QSAR) models for Human Immunodeficiency virus (HIV), Hepatitis B virus (HBV), Hepatitis C virus (HCV), and twenty-six other viruses (general viruses) which includes SARS coronavirus, and other respiratory viruses to predict the activity of an unknown compound (Qureshi et al., 2017).

Protein preparation

The crystal structures of NSP3, NSP7/8protein, and NSP9 with PDB IDs 6W02, 6WIQ, and 6WXD were retrieved from the protein databank (http://www.rcsb.org) (Littler et al., 2020; Michalska et al., 2020; Wilamowski et al., 2020). The structures were prepared individually by eliminating existing ligands and water molecules, while the absent hydrogen atoms were added using the Autodock v4.2 program, Scripps Research Institute (Goodsell et al., 1996). The search grid was expanded above the target proteins and the parameters of the atomic solution were determined. Polar hydrogen charges of the Gasteiger type were allocated and the non-polar hydrogens were integrated with the carbons and the internal degrees of freedom and torsion were formed. Target proteins were subsequently saved into pdbqt format in preparation for molecular docking.

Ligand preparation

The SDF structures of four selected histamine H2-receptor antagonists, i.e. Famotidine, Nizatidine, Cimetidine, and Ranitidine was obtained from the PubChem database (www.pubchem.ncbi.nlm.nih.gov). Using Open babel program (O'Boyle et al., 2011), the compounds were converted from SDF to mol2 chemical format. The ligand's alpha carbon was detected when the internal degrees of freedom and torsion were set to zero. Further, the compounds were converted using Autodock tools to a dockable pdbqt format.

Molecular docking

Docking of the four selected histamine H2-receptor antagonists to selected coronavirus targets as well as the assessment of binding affinities was done by using Vina GUI (Trott & Olson, 2010). The Pdb format of the proteins and the ligands were dragged into their respective columns. The grid center for docking was detected as $X = 0.49$, $Y = -0.12$, $Z = 0.68$ with the

Table 1. Antiviral activity of screened histamine H2-receptor antagonists showing percentage inhibition of various viruses.

S/N	Compounds	General virus	HBV	HCV	HHV	HIV
1	Cimetidine	63.62	31.54	16.98	45.78	63.23
2	Famotidine	59.51	21.08	59.53	49.45	44.23
3	Nizatidine	63.86	21.82	7.60	48.17	61.75
4	Ranitidine	54.77	23.92	15.34	37.59	66.92

dimensions of the grid box, $46.64 \times 58.51 \times 84.39$ for NSP3, X= -3.20, Y= -17.91, Z= -5.31 with the dimensions of the grid box, $45.09 \times 64.71 \times 60.69$ for NSP7/8 protein, and $X = 40.56$, Y= -11.50, $Z = 13.86$ with the dimensions of the grid box, $67.52 \times 56.99 \times 58.04$ for NSP9 protein. Subsequently, the software was run and cluster analysis based on Root Mean Square Deviation (RMSD) values for starting geometry was conducted and the lowest energy conformation of the more populated cluster was found to be the most accurate solution. The docking process was replicated three times for each compound.

The docking was revalidated using Blind Docking Server (Sánchez-Linares et al., 2012), a web-based tool that utilizes a modified version of Vina to sample across the whole protein surface to determine the best pose. In their respective columns, the Pdb forms of individual proteins and ligands were uploaded, and the online tool was run. Blind Docking Server uses exhaustive docking simulations on alpha carbon of the protein and it uses a clustering algorithm to detect new binding modes to measure binding energies. After the binding energies were calculated, the tool clustered the results according to the spatial overlapping of the resulted docking poses. The pose with the strongest affinity for each cluster was taken as the representation of this cluster. The compounds were then ranked by their affinity scores. Thereafter, molecular interactions between coronavirus targets and the compounds that have the highest binding affinity were viewed with Discovery Studio Visualizer, 2020 (Dassault, 2020).

Molecular dynamics simulation

For analyzing the structural stability of Nsps, Nsp-Cimetidine complexes, and Nsp-Famotidine complexes, molecular dynamics simulations (MDS) were conducted using GROMACS 5.0 (Pronk et al., 2013) package. The MD simulations were executed on a workstation with configuration Ubuntu 16.04 LTS 64-bit, 4 GB RAM, Intel ®CoreTM i5-6400 CPU. We performed three times replicated, 100 ns-scale MD simulations for each studied complex. Total twenty one systems (three Apo protein, i.e. Nsp3, Nsp7/8, Nsp9, and eighteen protein-ligand complex, i.e. three Nsp3-Cimetidine complexes (Nsp3-C1, Nsp3-C2 and Nsp3-C3 complex), three Nsp3-Famotidine complexes (Nsp3-F1, Nsp3-F2 and Nsp3-F3 complex), three Nsp7/8-Cimetidine complexes (Nsp7/8-C1, Nsp7/8-C2 and Nsp7/8-C3 complex), three Nsp7/8-Famotidine complexes (Nsp7/8-F1, Nsp7/8-F2 and Nsp7/8-F3 complex), three Nsp9-Cimetidine complexes (Nsp9-C1, Nsp9-C2 and Nsp9-C3 complex), and three Nsp9-Famotidine complexes (Nsp9-F1, Nsp9-F2 and Nsp9-F3 complex) were created and subjected to 100 ns Molecular Dynamics Simulation studies. The topologies for protein as well as protein-ligand

complexes were prepared by using the CHARMM36 force field (Vanommeslaeghe et al., 2009). After that, ligand topologies were attached to the processed protein structure to create a complex protein-ligand structure. The topology file includes all details like non-bonded parameters as well as bonded parameters such as atom forms, charges, and bonded connectivity etc. Compounds to be simulated must be immersed in solvation medium like water and other solvents to mimic the cellular environment. Therefore, using the TIP3P water model (Izadi & Onufriev, 2016) with dodecahedral periodic boundary conditions, a water solvated system was built. After solvation, Na^+ counter-ions were added to neutralize all the systems by using the 'gmx genion' script. Further, the energy minimization process was run to ensure that the complexes have no steric clashes and a reasonable starting structure. Energy minimization was accomplished with the steepest descent algorithm by using Verlet cut-off scheme. In two phases, the equilibration of the system was attained. Equilibration under the NVT ensemble was carried out at 300 K for 10 ps thereby stabilizing the temperature of the system. The second phase was run under an NPT ensemble, followed by a 10 ps NPT simulation at 1 atm. The systems were subjected at a constant temperature (300 K) and constant pressure (1 atm) with a time step of 2 fs, using the Parrinello-Rahman for constant pressure simulation. At last, the production MD of the protein and protein-ligand complexes was carried out for 100 ns. After successful execution of MD, for analyzing the stability of protein and protein-ligand complex system, Root mean square fluctuation (RMSF), Root-mean square deviation (RMSD), Radius of Gyration (RG), hydrogen bonds, Principle component analysis (PCA), Solvent Accessible Surface Area (SASA) were calculated. The number of distinct hydrogen bonds formed within the complex and protein during the simulation was calculated by hydrogen bond analysis.

Binding free energy calculation using MM-PBSA

The binding free energy estimation provides a quantitative estimation of interactions between protein and ligand that help to understand the stability of that protein-ligand complex (Kumari et al., 2014). The MMPBSA (Molecular Mechanics Poisson-Boltzmann Surface Area) approach is commonly used for measuring the binding free-energy to estimate the stability of the protein-ligand complex following MD simulation. The binding free energy includes free solvation energy (polar and nonpolar solvation energies) and potential energy (electrostatic and Vander Waals interactions). Here, binding free energy calculations of Nsp-Cimetidine complexes and Nsp-Famotidine complexes were done by the MMPBSA method. The MD trajectories were processed before the measurement of binding free energy. Then average binding energy calculations were done with the 'python' script provided in g_mmpbsa.

Gene target prediction

Identification of potential target genes for Cimetidine and Famotidine was carried out using the HitPickV2 server (Hamad et al., 2019) using their respective smiles string. The upstream
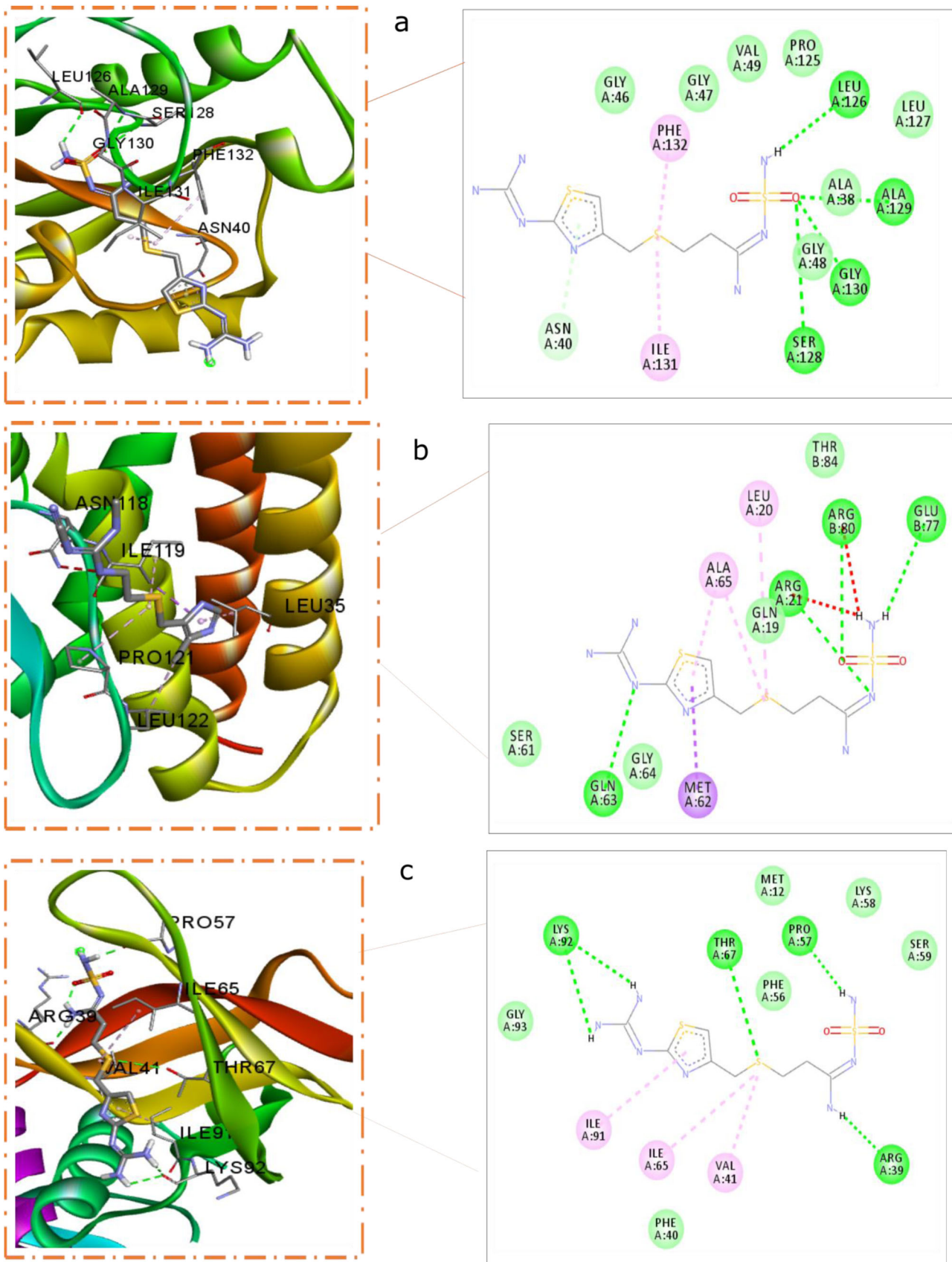
Figure 1. Binding of Famotidine to non-structural proteins, (a) Famotidine binding to NSP3 binding site, (b) Famotidine binding to NSP7-8 complex, (c) Famotidine binding to NSP9 complex.

regulatory networks from signatures of differentially expressed genes obtained from Cimetidine and Famotidine target prediction were determined by transcription factor enrichment analysis, protein-protein interaction network expression and kinase enrichment analysis using eXpression2Kinases (X2K) Web server (Clarke et al., 2018).

Table 2. Binding affinity of H2RAs to coronavirus proteins.

		Vina's score ΔG (kcal/mol)									BINDSURF's score ΔG (kcal/mol)		
		NSP3			NSP7NSP8			NSP9			NSP3	NSP7/8 complex	NSP9
SN	Compounds	I	II	III	I	II	III	I	II	III			
1	Cimetidine	−6.2	−6.1	−6.2	−6.3	−6.1	−6.2	−5.1	−4.8	−4.9	−7.7	−6.2	−6.3
2	Famotidine	−6.4	−6.7	−6.4	−6.4	−6.6	−6.6	−5.1	−4.8	−5.3	−9.2	−7.0	−7.5
3	Nizatidine	−6.0	−5.8	−5.6	−6.0	−6.0	−5.6	−4.3	−4.1	−4.4	−7.1	−6.0	−6.5
4	Ranitidine	−6.2	−6.2	−6.0	−6.2	−6.2	−6.1	−4.7	−4.5	−4.6	−7.3	−5.9	−6.4

I, II, and III indicates the first, second and third docking result since the docking performed triplet.

Table 3. Hydrogen and non-hydrogen bond interaction between histamine H2-receptor antagonists and coronavirus proteins.

		NSP3		NSP7/8 complex		NSP9	
S/N	Compounds	H-bond	Non H-bond	H-bond	Non H-bond	H-bond	Non H-bond
1	Cimetidine	Ala38, Gly48, Ala151	Leu126, Phe132, Val155	Ile32, Phe132, Ala154	Ile131	Leu9, Tyr31, Ala105, Thr109,	–
2	Famotidine	Leu126, Ser128, Ala129, Gly130	Ile131, Phe132	Arg21, Gln63, Glu77, Arg80	Leu20, Met62, Ala65,	Arg39, Pro57, Thr67, Lys92	Val41, Ile65, Ile91
3	Nizatidine	Lys55	Asp22, Glu25, Val49, Phe156	Gln63	Asp67, Pro133, Pro183	Thr24, Gly38, Arg39, Ser59	Phe56
4	Ranitidine	Lys55, Leu126	Asp22, Val49	Gln63	Asp67, Pro133, Pro183	Arg39, Pro57, Ser59, Lys92,	Lys58, Thr67

Results and discussion

Anti-viral activity prediction

All H2RAs showed good anti-viral activity against several viruses generally with Cimetidine (63.62%) and Nizatidine (63.82) being the most potent followed by Famotidine (59.51%) and the least being Ranitidine (54.77%) (Table 1). However, the compound showed specificity for different viruses, with Famotidine being remarkable for HCV (59.53%) and HHV (49.45) compared to other compounds. Moreover, other compounds are more specific for HIV with over 60% inhibitory activity compared to Famotidine's (44.23%). Although all compounds showed a poor activity towards HBV with less than 35% activity. The ability of this compound to inhibit a broad spectrum of viruses may be useful in the diagnosis of coronavirus diseases. The percentage inhibition obtained indicates that all the compounds can be used to develop antiviral drugs to treat viral infections.

Molecular docking of the ligands to selected non-structural proteins

Molecular docking of H2RAs to coronavirus proteins revealed that Famotidine and Cimetidine had a higher binding affinity to all proteins studied. Docking process was performed three times for each ligand using the same coordinates and in each time the results were almost very similar. The Famotidine showed the binding energy of −6.4, −6.7, and −6.4 kcal/mol to NSP3, −6.4, −6.6, and −6.6 kcal/mol to NSP7/8 complex, −5.1, −4.8, and −5.3 kcal/mol to NSP9 during docking replications, whereas Cimetidine showed −6.2, −6.1, and −6.2 kcal/mol to NSP3, −6.3, −6.1, and −6.2 kcal/

mol to NSP7/8 complex, and 5.1, −4.8, and −5.3 kcal/mol to NSP9, respectively, compared to other compounds (Table 2).

Also, BINDSURF confirmed the superiority of Famotidine (with a binding affinity of −9.2, −7.0, and −7.5 kcal/mol for NSP3, NSP7/8 complex, and NSP9) and Cimetidine (with a binding affinity of −5.6, −6.2, and −6.3 kcal/mol for NSP3, NSP7/8 complex, and NSP9) compared to other H2RAs. Other H2Ras had a relatively lower binding affinity for the three proteins compared to Famotidine and Cimetidine.

Famotidine was visualized in predominantly major hydrogen bond formation with Leu126, Ser128, Ala129, and Gly130 of NSP3 (Figure 1a). Hydrophobic interactions with Ile131 and Phe132 were also visible. The Famotidine-NSP7/8 complex involved multiple hydrogen bond formation with Arg21, Gln63, Glu77, and Arg80 (Figure 1b). Arg39, Pro57, Thr67, and Lys92 of NSP9 interacted with Famotidine via hydrogen bond in addition to hydrophobic interactions with Val41, Ile65, and Ile91 (Figure 1c and Table 3).

A combination of hydrogen bond with Gly48, Ala-residues at positions 38 and 154 and hydrophobic interactions with Leu126, Val155 (π-alkyl), and Phe132 (π-sigma interaction) were visualized in the binding of Cimetidine to Nsp3 (Figure 2a). Cimetidine binds to the Nsp7/8 complex via a hydrogen bond with Ile23, Ala154, and a π-alkyl interaction with Ile131 (Figure 2b). The binding of Cimetidine to Nsp9 revealed a multiple hydrogen bond formation with Leu9, Tyr31, Ser105, and Thr109 in the binding site of Nsp9 (Figure 2c).

As the largest non-structural protein of CoVs, Nsp3 has been regarded as the primary selective target for driving evolution in lineage C β-coronaviruses based on a high rate of positively selected mutation sites (Forni et al., 2016).
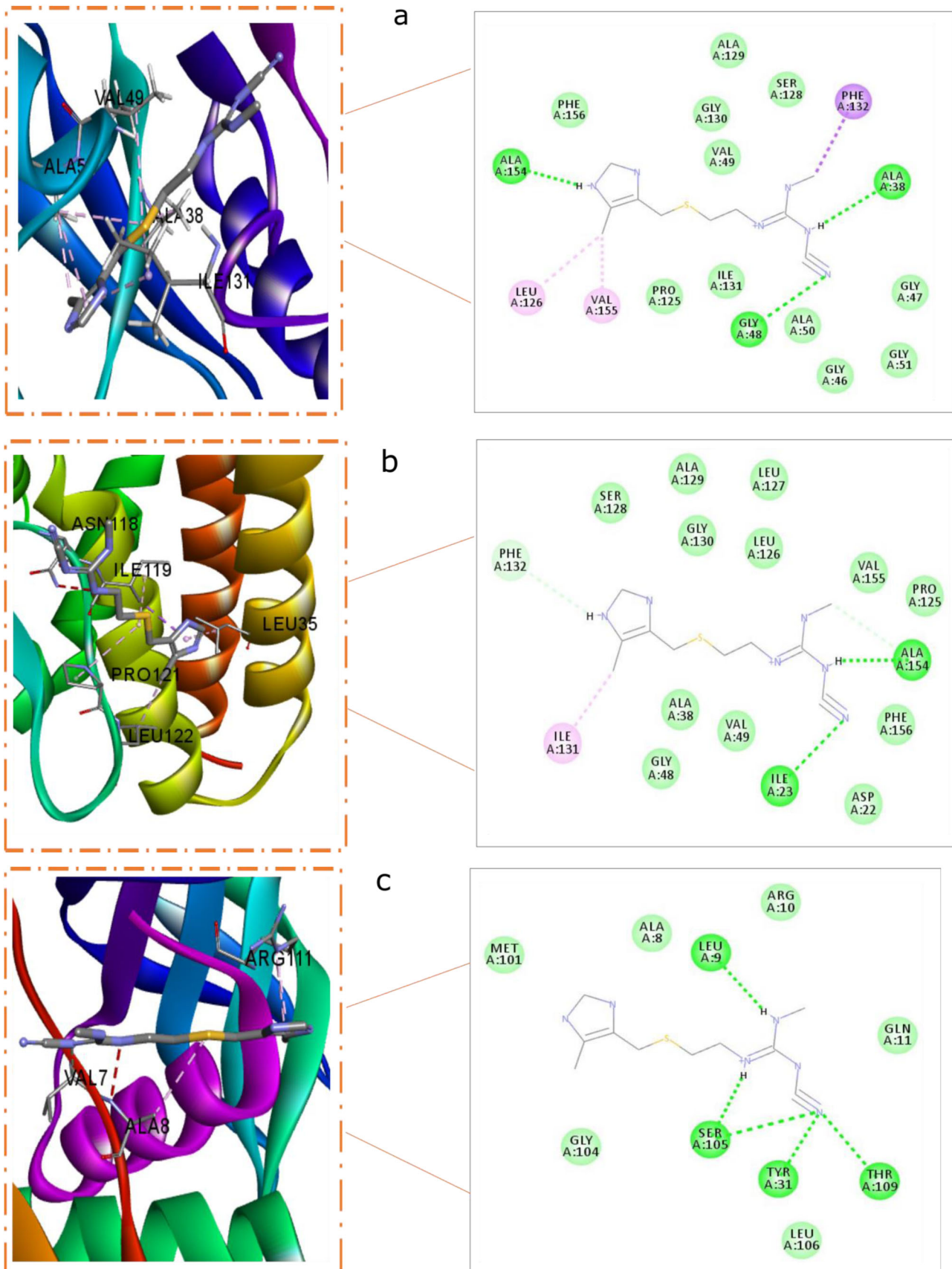
Figure 2. Binding of Cimetidine to non-structural proteins, (a) Cimetidine binding to NSP3 binding site, (b) Cimetidine binding to NSP7-8 complex, (c) Cimetidine binding to NSP9 complex.

Table 4. The average values of RMSD, RMSF, RG, SASA, H-bond and Gibbs energy in Nsp proteins, Nsp-Cimetidine complexes, and Nsp-Famotidine complexes.

S. No.	Protein/Protein-ligand complex	Average RMSD (nm)	Average RMSF (nm)	Average RG (nm)	Average SASA (nm²)	H-bond	Gibbs energy (kJ mol⁻¹)
1	Nsp3-protein	0.09 ± 0.01	0.07 ± 0.03	1.21 ± 0.06	–	–	–
2	Nsp3-C1 complex	0.10 ± 0.01	0.06 ± 0.02	1.15 ± 0.06	84.71 ± 2.06	2–4	11.9
3	Nsp3-C2complex	0.11 ± 0.01	0.06 ± 0.02	1.23 ± 0.05	83.13 ± 1.16	3–5	12.6
4	Nsp3-C3 complex	0.11 ± 0.02	0.06 ± 0.03	1.16 ± 0.07	83.51 ± 1.42	2–4	13.1
5	Nsp3-F1 complex	0.09 ± 0.01	0.67 ± 0.03	1.19 ± 0.07	85.63 ± 2.42	4–8	13
6	Nsp3-F2 complex	0.09 ± 0.01	0.06 ± 0.02	1.14 ± 0.06	85.78 ± 1.94	6–8	12.6
7	Nsp3-F3 complex	0.11 ± 0.01	0.06 ± 0.02	1.16 ± 0.06	83.58 ± 1.35	2–5	11.3
8	Nsp7/8 protein	0.10 ± 0.01	0.06 ± 0.02	1.18 ± 0.07	–	–	–
9	Nsp7/8-C1 complex	0.96 ± 0.01	0.06 ± 0.02	1.17 ± 0.06	87.76 ± 2.08	2–5	13.1
10	Nsp7/8-C2 complex	0.99 ± 0.01	0.06 ± 0.02	1.19 ± 0.06	86.29 ± 2.68	2–5	12.7
11	Nsp7/8-C3 complex	0.10 ± 0.01	0.06 ± 0.03	1.18 ± 0.06	82.62 ± 1.31	2–5	13.4
12	Nsp7/8-F1 complex	0.09 ± 0.01	0.06 ± 0.02	1.21 ± 0.06	85.16 ± 2.03	3–6	12.7
13	Nsp7/8-F2 complex	0.10 ± 0.02	0.02 ± 0.03	1.21 ± 0.07	86.13 ± 2.14	6–8	12.7
14	Nsp7/8-F3 complex	0.10 ± 0.01	0.06 ± 0.02	1.20 ± 0.07	85.67 ± 2.61	4–7	13.7
15	Nsp9 protein	0.35 ± 0.07	0.12 ± 0.11	1.20 ± 0.07	–	–	–
16	Nsp9-C1 complex	0.35 ± 0.08	0.16 ± 0.15	1.14 ± 0.07	77.62 ± 02.81	1–3	14.9
17	Nsp9-C2 complex	0.32 ± 0.06	0.16 ± 0.12	1.16 ± 0.08	76.34 ± 1.94	2–6	12.2
18	Nsp9-C3 complex	0.32 ± 0.08	0.16 ± 0.15	1.15 ± 0.08	76.52 ± 3.17	4–6	14.1
19	Nsp9-F1 complex	0.36 ± 0.11	0.19 ± 0.18	1.13 ± 0.08	77.77 ± 2.69	3–6	14.6
20	Nsp9-F2 complex	0.29 ± 0.07	0.16 ± 0.15	1.18 ± 0.08	75.48 ± 3.13	4–7	11.8
21	Nsp9-F3 complex	0.38 ± 0.08	0.21 ± 0.18	1.18 ± 0.08	79.58 ± 2.63	4–9	11.9
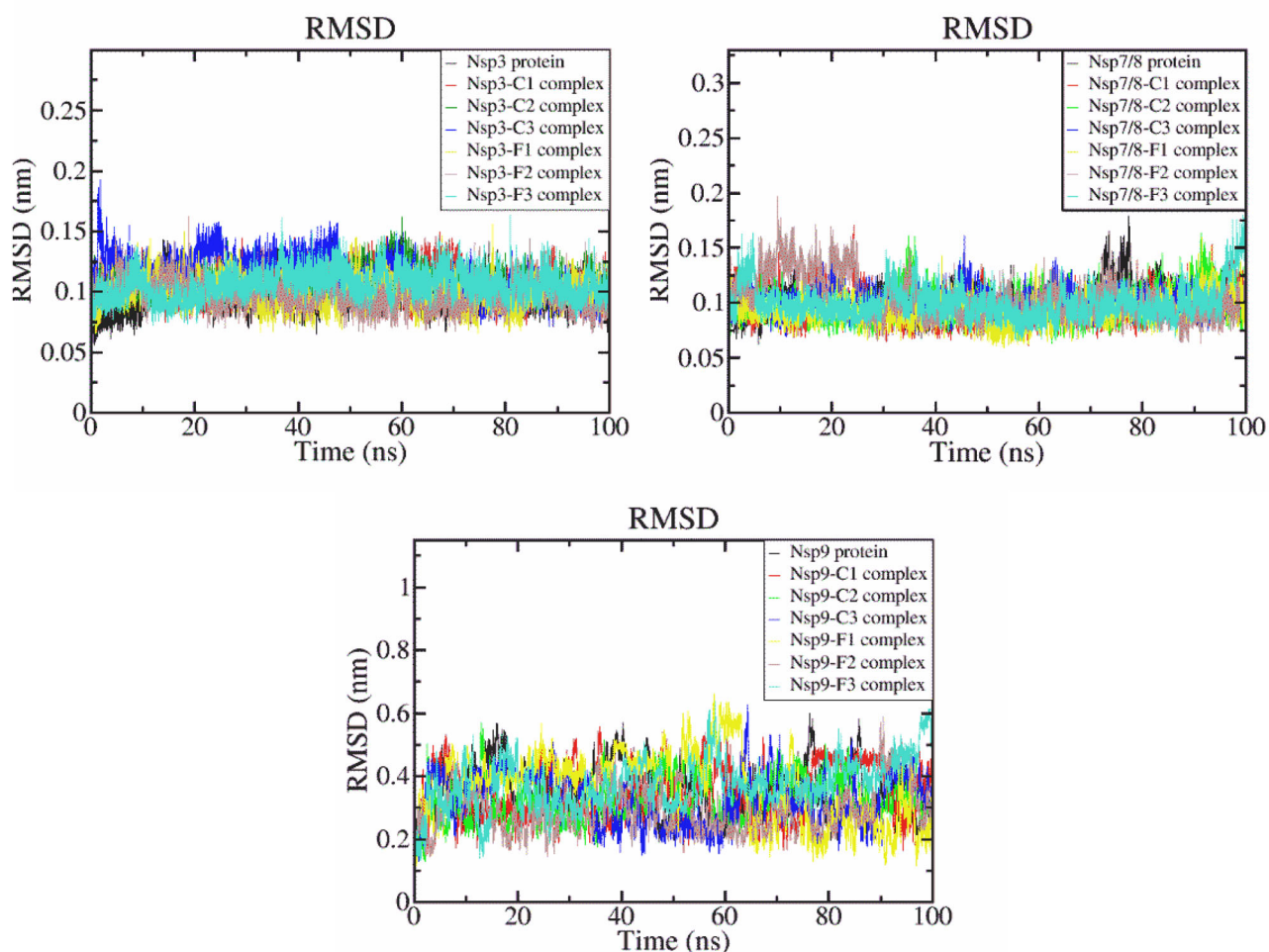
Figure 3. RMSD study plots of native Nsp proteins, Nsp-Cimetidine complexes (Nsp-C1, Nsp-C2, Nsp-C3 complex), and Nsp-Famotidine complexes (Nsp-F1, Nsp-F2, Nsp-F3 complex) during 100 ns of MD simulations.

Cimetidine and Famotidine's ability to bind NSP3 may prevent the protein from acting as a scaffold thereby preventing interaction with itself and other viral NSPs in the process halting viral replication. Also, Cimetidine and Famotidine binding with NSP7-8 heterodimer may disrupt its binding to NSP12 thereby preventing the formation of RNA polymerase complex. Nsp9 dimerizes in a solution using a conserved α-helical 'GxxxG' motif (Sutton et al., 2004). The Famotidine
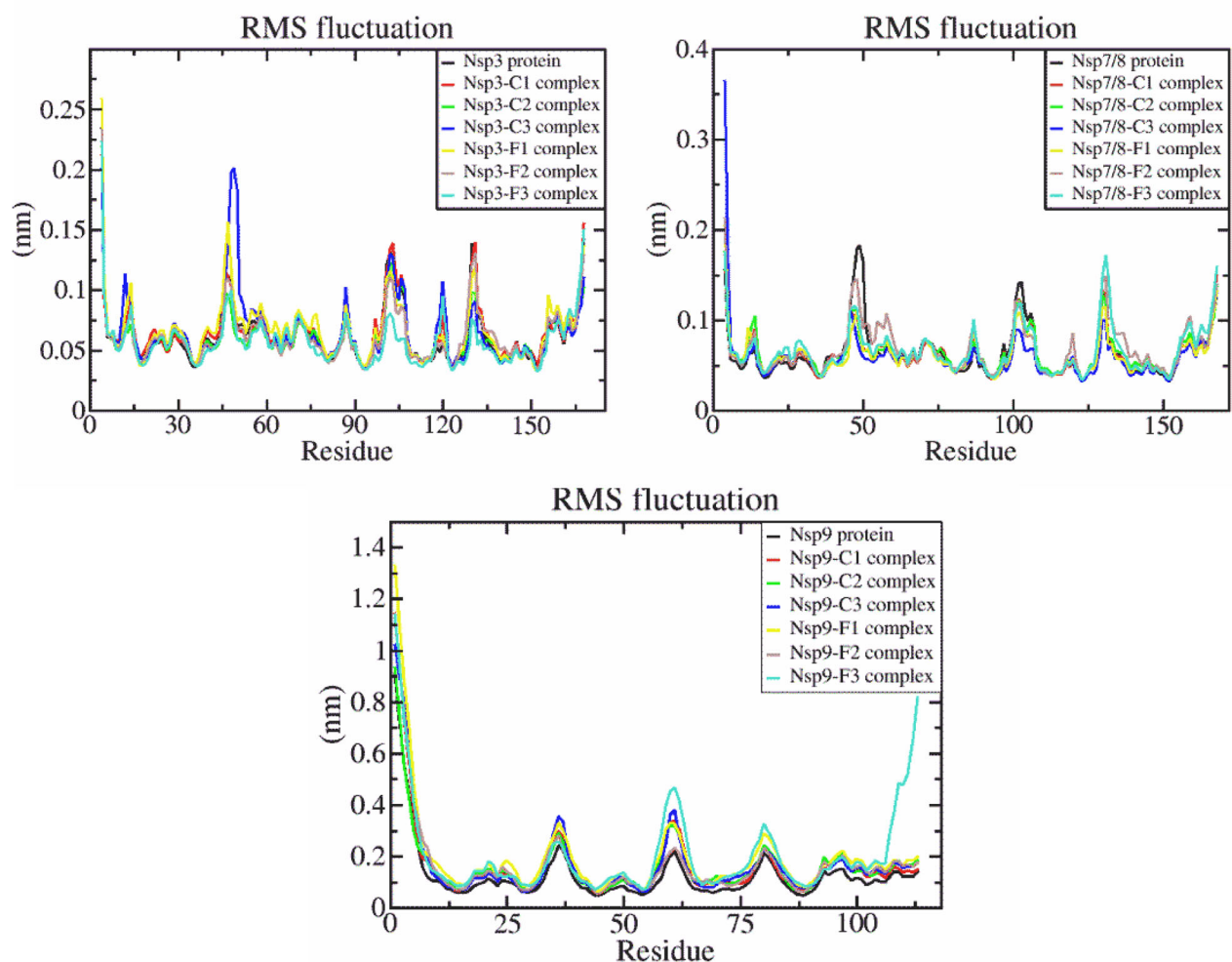
Figure 4. The graphs reflecting the RMSF values of Ca atoms for Nsp proteins, Nsp-Cimetidine complexes (Nsp-C1, Nsp-C2, Nsp-C3 complex), and Nsp-Famotidine complexes (Nsp-F1, Nsp-F2, Nsp-F3 complex).

binding could disrupt key residues in this motif and reduce both RNA binding and SARS-CoV-2 viral replication.

Molecular dynamics simulation

The MDS was performed for predicting the stability of the Nsp proteins, Nsp-Cimetidine complexes, and Nsp-Famotidine complexes. The structural changes and dynamic behavior in Nsp proteins, Nsp-Cimetidine complexes, and Nsp-Famotidine complexes were analyzed by the various computational analyses like RMSD, RMSF, RG calculation, and values are shown in Table 4.

Root mean square deviation (RMSD)

The RMSD analysis monitored the conformational as well as the structural stability of Nsp proteins Nsp-Cimetidine complexes, and Nsp-Famotidine complexes. Through RMSD analysis, we observed the variations between the backbone atoms of native proteins from the original conformation to their final position. The stability of any conformation is defined by the deviations that occurred during the simulation. The smallest deviation indicates the good stability of the structure. For the 100 ns simulation, the RMSD value of the C-alpha backbone was calculated.

Figure 3 illustrates the RMSD (nm) versus time (ns) plots for native Nsp proteins, Nsp-Cimetidine complexes, and Nsp-Famotidine complexes. From this calculation, we have observed that all complexes are stable and have developed stable structures for further assessment. Table 4 displays the average RMSD values for all systems. The native Nsp3 showed stability within the 100 ns trajectory with an average RMSD of 0.09 nm, while the average RMSD of Nsp3-Cimetidine and Nsp3-Famotidine complexes was 0.10–0.11 nm and 0.09–0.11 nm, respectively. Similarly, the native Nsp7/8 protein, Nsp7/8-Cimetidine, and Nsp7/8-Famotidine complexes were relatively stable throughout the simulation (Figure 3) with an average RMSD of 0.10, 0.96–0.10 nm and 0.09–0.10 nm, respectively. The native Nsp9 protein, Nsp9-Cimetidine, and Nsp9-Famotidine complexes were relatively stable throughout the simulation (Figure 3) with an average RMSD of 0.35 nm, 0.32–0.35 nm and 0.29–0.38 nm, respectively. Overall, the RMSD fluctuation results show that the MD trajectories are relatively stable and were within an acceptable range for all the studied complexes during the simulation time.

Root mean square fluctuation (RMSF)

Conformational variations of the native Nsp proteins and residues that participated in the interactions of Nsp-Cimetidine
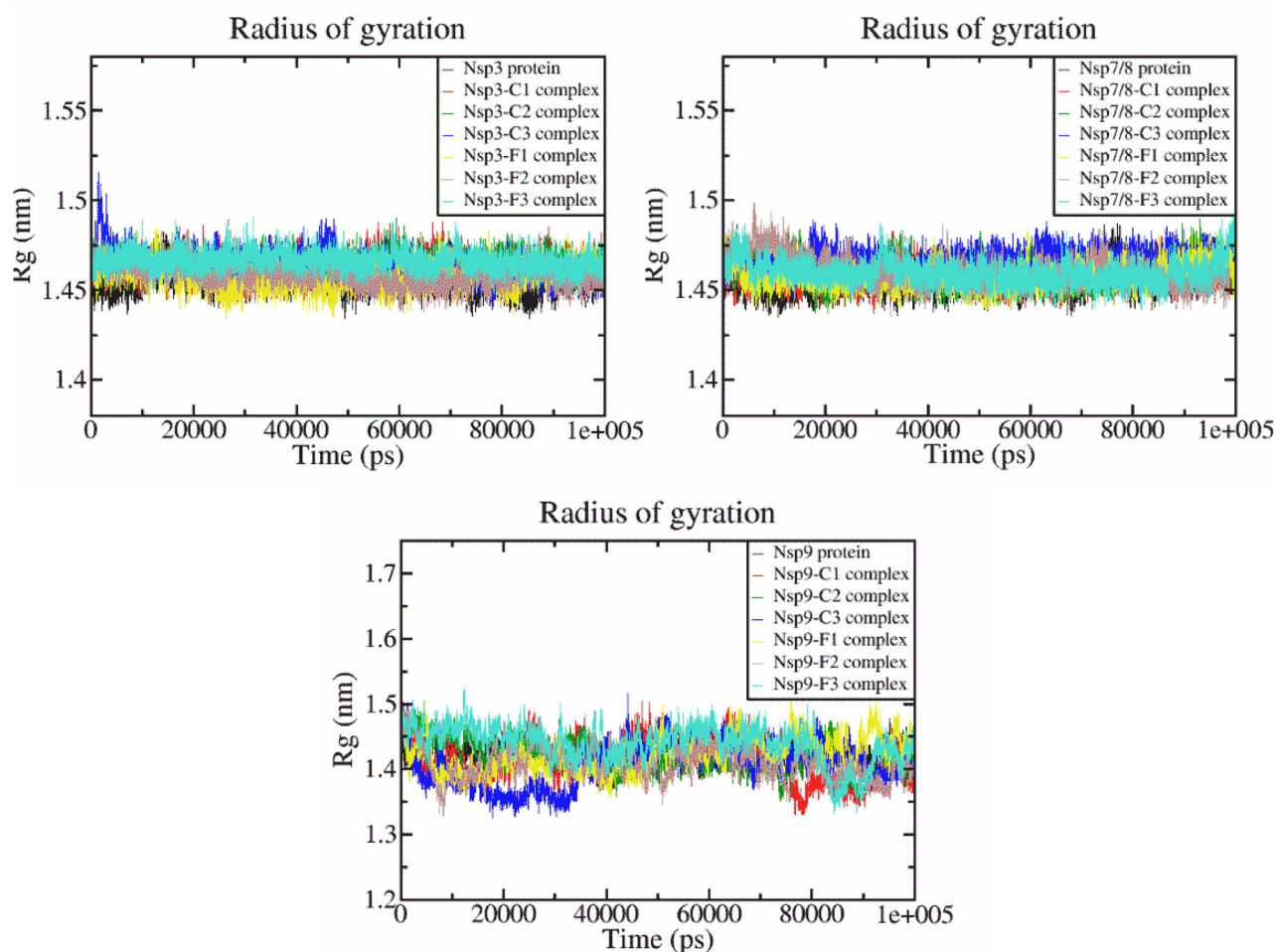
Figure 5. Radius of gyration plots reflecting the changes observed in the conformational behavior of the Nsp proteins, Nsp-Cimetidine complexes (Nsp-C1, Nsp-C2, Nsp-C3 complex), and Nsp-Famotidine complexes (Nsp-F1, Nsp-F2, Nsp-F3 complex).

complexes and Nsp-Famotidine complexes were determined by RMSF analysis. RMSF analyses amino acid residues that fluctuate in the overall structure or indicates dynamic regions of the protein. Higher RMSF values imply higher flexibility or lower stability, whereas the lower RMSF value shows the strong stability of the complex during the MD simulation. During the 100 ns trajectory, fluctuations in the constituent residues were observed and plotted to compare the flexibility of each residue in the native Nsp proteins and their respective complexes (Figure 4). The RMSF plot reveals that the secondary structure of Nsp proteins, Nsp-Cimetidine complexes, and Nsp-Famotidine complexes remains stable throughout the MD simulation. The Nsp9 protein as well as both Nsp9 complexes yielded little fluctuations at Gly37, Gly61, and Pro80 residues. Otherwise, the fluctuation during all protein-ligand interactions was below 0.2 nm which is perfectly acceptable. The average RMSF values for all Nsp proteins and all Nsp complexes are shown in Table 4. In conclusion, it indicated that RMSF of all Nsp-Cimetidine complex and Nsp-Famotidine complexes are significantly similar to Nsp-proteins resulting in less fluctuation and good stability.

Radius of gyration (Rg)

The Rg is an effective parameter to understand the level of compaction in the structure of the protein in the absence and

presence of ligand. Rg is used to evaluate if the complexes will be stably folded or unfolded during the MD simulation. Higher Rg value indicates lower compactness of the protein-ligand complex. The time evolution plots of Rg for all Nsp proteins, all Nsp3-Cimetidine complexes, and Nsp-Famotidine complexes are shown in Figure 5. If the protein is likely to retain a relatively stable Rg value in the MD simulation, it can be considered stably folded, and it can be considered unfolded if its Rg changed over time. All the Nsp-Famotidine complexes showed relatively similar and stable values of Rg as the corresponding Nsp protein, which reveals that they are ideally superimposed with each other and demonstrate comparable compactness and excellent stability (Table 4). These findings demonstrate that all complexes maintained relatively stable folded conformation over the 100 ns MD Simulation trajectory at a constant temperature of 300 K and a constant pressure of 1 atm. Overall, it can be inferred that the complexation of Nsp proteins with both Cimetidine and Famotidine increases the compactness/rigidity of the protein structure, leading to increased overall stability.

Post MD-simulation

Hydrogen bonds
The receptor-ligand complexes are stabilized by various types of interactions such as hydrogen bonding, hydrophobic
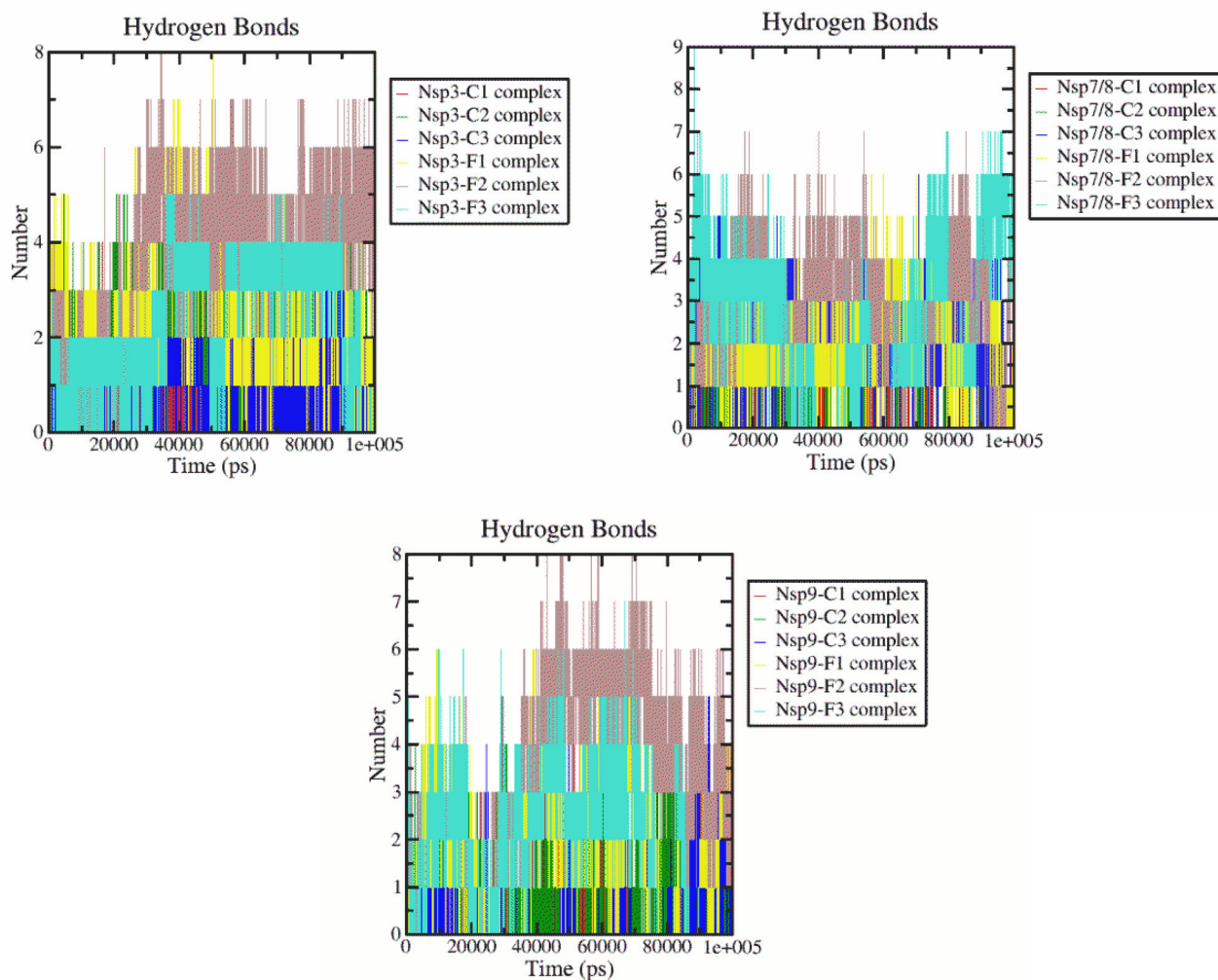
Figure 6. The 2-D diagram describing the dynamics observed in the hydrogen bonding patterns for all Nsp-Cimetidine complexes (Nsp-C1, Nsp-C2, Nsp-C3 complex), and Nsp-Famotidine complexes (Nsp-F1, Nsp-F2, Nsp-F3 complex) with Nsp proteins.

bonds, electrostatic and other interactions, but out of them, the hydrogen bonds are very specific interactions that play a crucial role in strengthening the protein-ligand complex. These are also responsible for the precision, development, and adsorption of drugs in the drug design process. The maximum number of hydrogen bonds formed between each Nsp-Cimetidine complexes and Nsp-Famotidine complexes were also investigated during the 100 ns MD simulation (Figure 6). The result shows the appearance of four to five and five to eight H-bond interactions in the Nsp3-Cimetidine complexes and Nsp3-Famotidine complexes, respectively, during the Simulation period. Similarly, three to six and six to nine H-bonds were observed in the Nsp9-Cimetidine complexes and Nsp9-Famotidine complexes, respectively, while the Nsp7/8-Cimetidine complexes and Nsp7/8-Famotidine complexes showed five and six to eight H-bonds, respectively (Table 4). These observed bonding parameters indicated that Cimetidine and Famotidine were bound to all Nsp proteins effectively and tightly.

Solvent accessible surface area (SASA)
The SASA analysis tells about the proportion of the protein surface that can be accessed by the water solvent and to

examine interactions between the complex and the solvent during Simulation analysis. So, we reported SASA values for Nsp-Cimetidine complexes and Nsp-Famotidine complexes. Figure 7 indicates the SASA value vs. time plot for all Nsp complexes. The average value of SASA is signified in Table 4. These calculations revealed that all Nsp-Cimetidine complexes and Nsp-Famotidine complexes had a substantially identical SASA value with particular Nsp protein during 100 ns MD simulation, suggesting no major differences in protein structure.

Principal component analysis (PCA)
PCA determines the most important components in dynamics trajectory which are responsible for protein movement. To perform PCA, the eigenvectors, and eigenvalues are calculated and projections of the eigenvalues and eigenvectors are evaluated using the essential dynamics (ED) approach. This is well recognized that just the first few eigenvectors determine the protein's overall motion. The diagonalization of the matrix is used to evaluate the eigenvectors. The first 40 eigenvectors were chosen in this analysis to measure the concerted motions. A set of eigenvectors was calculated by diagonalizing the matrix. The movements for the first ten eigenvectors accounted for 56.54 percent, 52.70 percent, and 59.28 percent
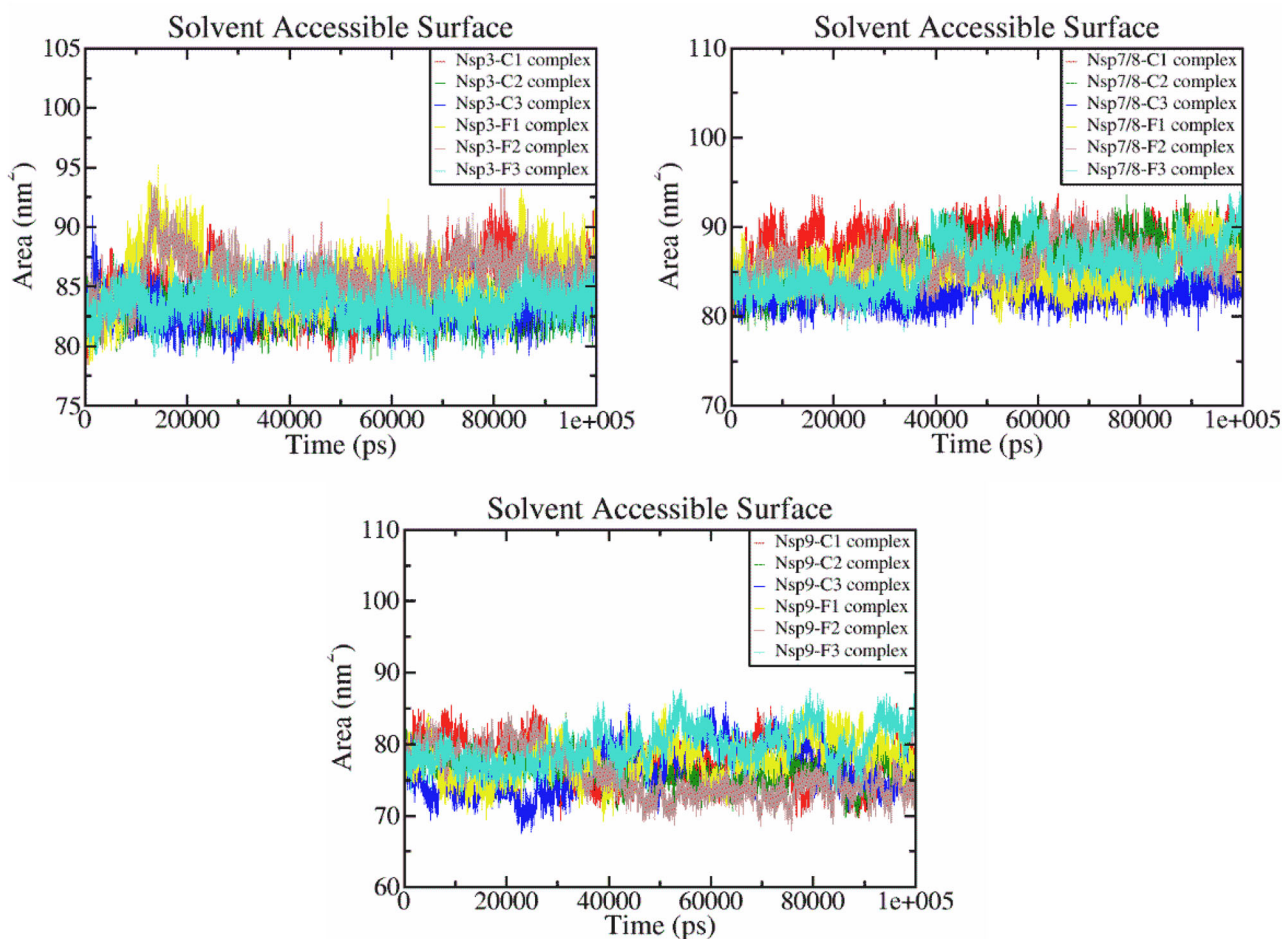
Figure 7. Solvent accessible surface area (SASA) value vs. time at 300 K for all Nsp-Cimetidine complexes (Nsp-C1, Nsp-C2, Nsp-C3 complex), and Nsp-Famotidine complexes (Nsp-F1, Nsp-F2, Nsp-F3 complex).

of the overall movements in Nsp3-Cimetidine complexes; 58.89 percent, 54.92 percent, and 50.27 percent of the overall movements in Nsp3-Famotidine complexes; 54.20 percent, 54.95 percent, and 56.07 percent of the overall movements in Nsp7/8-Cimetidine; 52.70 percent, 61.68 percent, and 59.10 percent of the overall movements in Nsp7/8-Famotidine; 89.06 percent, 85.22 percent, and 89.84 percent of the overall movements in Nsp9-Cimetidine complexes; 92 percent, 90.48 percent, and 90.79 percent of the overall movements in Nsp9-Famotidine complexes, respectively, during 100 ns simulation time (Figure 8a). So from the PCA, we conclude that Cimetidine and Famotidine has fewer movements and establishes a stable complex with all Nsp proteins.

The dynamics of studied complexes was also accomplished by 2-dimensional plot creation in PCA (Figure 8b). Figure 8(b) displays the 2-dimensional projection of MD trajectories in phase space for the first two principal components, i.e. PC1 and PC2 for Nsp-Cimetidine complexes and Nsp-Famotidine complexes. The complex which occupies less phase space and the stable cluster indicates a more stable complex, while the complex taking more space is a non-stable cluster which indicates a less stable complex. From the figure, it can be observed that the Nsp3-Cimetidine, Nsp3-Famotidine, Nsp7/8-Cimetidine, and Nsp7/8-Famotidine complexes were highly stable because they occupied less phase space, and the cluster was well established

except the Nsp9-Cimetidine and Nsp9-Famotidine complex. All results indicate that Nsp3-Cimetidine, Nsp3-Famotidine, Nsp7/8-Cimetidine, and Nsp7/8-Famotidine complexes are more stable complexes as compared to the Nsp9-Cimetidine and Nsp9-Famotidine complexes.

The Gibbs energy landscape plot for PC1 and PC2 was also calculated and is shown in Figure 9(A)–(F). The plot shows Gibbs energy values ranging from 0 to 11.9, 0 to 12.6, and 0 to 13.1 kJ mol^{-1} for Nsp3-Cimetidine complexes, 0 to 13, 0 to 12.6, and 0 to 11.3 kJ mol^{-1} for Nsp3-Famotidine complexes, 0 to 13.1, 0 to 12.7, and 0 to 13.4 kJ mol^{-1} for Nsp7/8-Cimetidine complexes, 0 to 12.7, 0 to 12.7, and 0 to 13.7 kJ mol^{-1} for Nsp7/8-Famotidine complexes, 0 to 14.9, 0 to 12.2, and 0 to 14.1 kJ mol^{-1} for Nsp9-Cimetidine complexes, and 0 to 14.6, 0 to 11.8, and 0 to 11.9 kJ mol^{-1} for Nsp9-Famotidine complexes, respectively. All the studied complexes showed significantly similar energy, which suggests that these complexes follow the energetically more favorable transition from one conformation to another and were thermodynamically favorable.

Binding energy calculation and energetic contribution of individual residues

The Binding energy calculation was performed using the MM-PBSA method implemented in GROMACS for all Nsp-
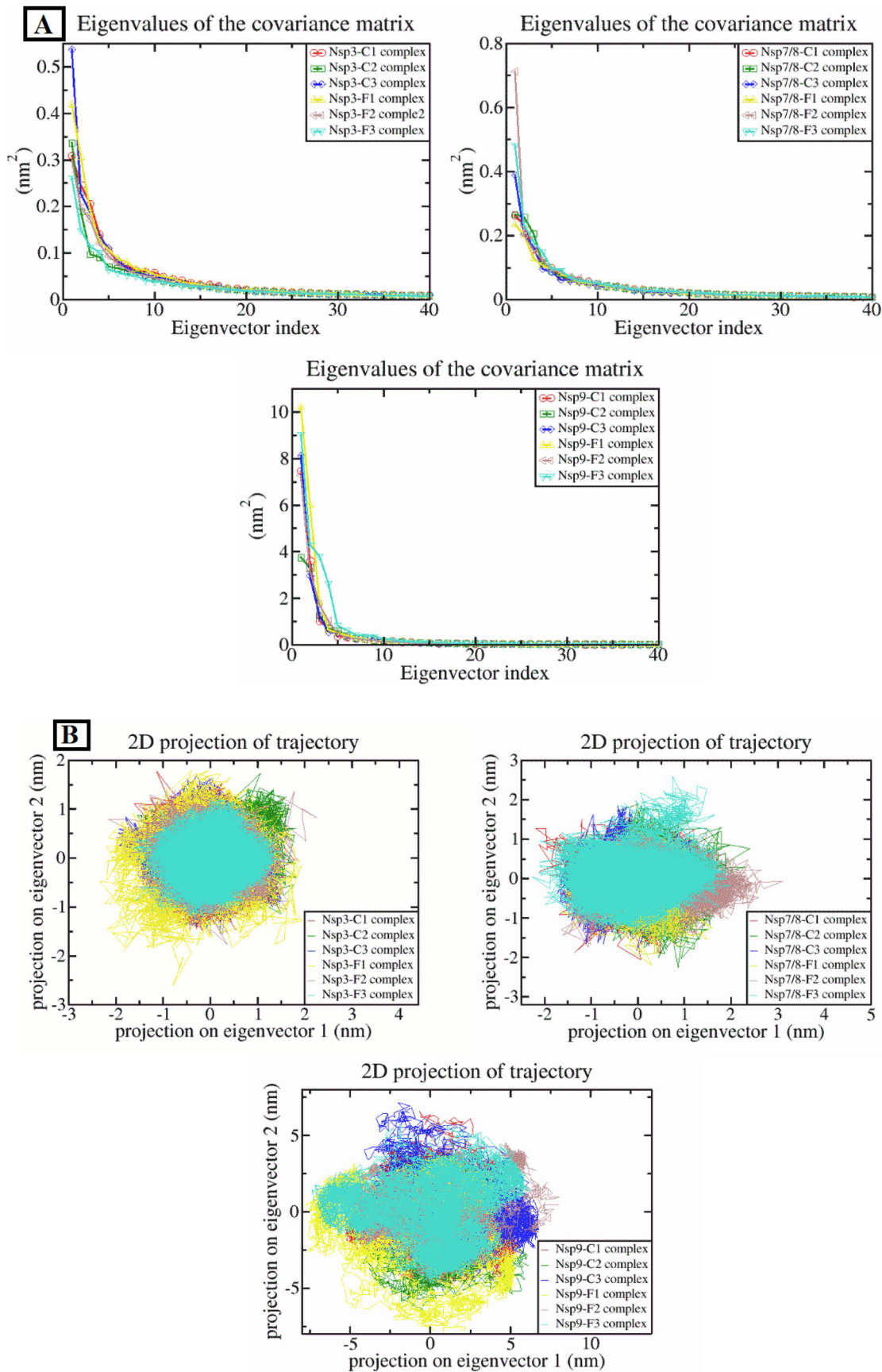
Figure 8. Principal component analysis. (A) The plot of eigenvalues vs. first 40 eigenvectors, (B) First two eigenvectors describing the protein motion in phase space for all Nsp-Cimetidine complexes (Nsp-C1, Nsp-C2, Nsp-C3 complex), and Nsp-Famotidine complexes (Nsp-F1, Nsp-F2, Nsp-F3 complex).
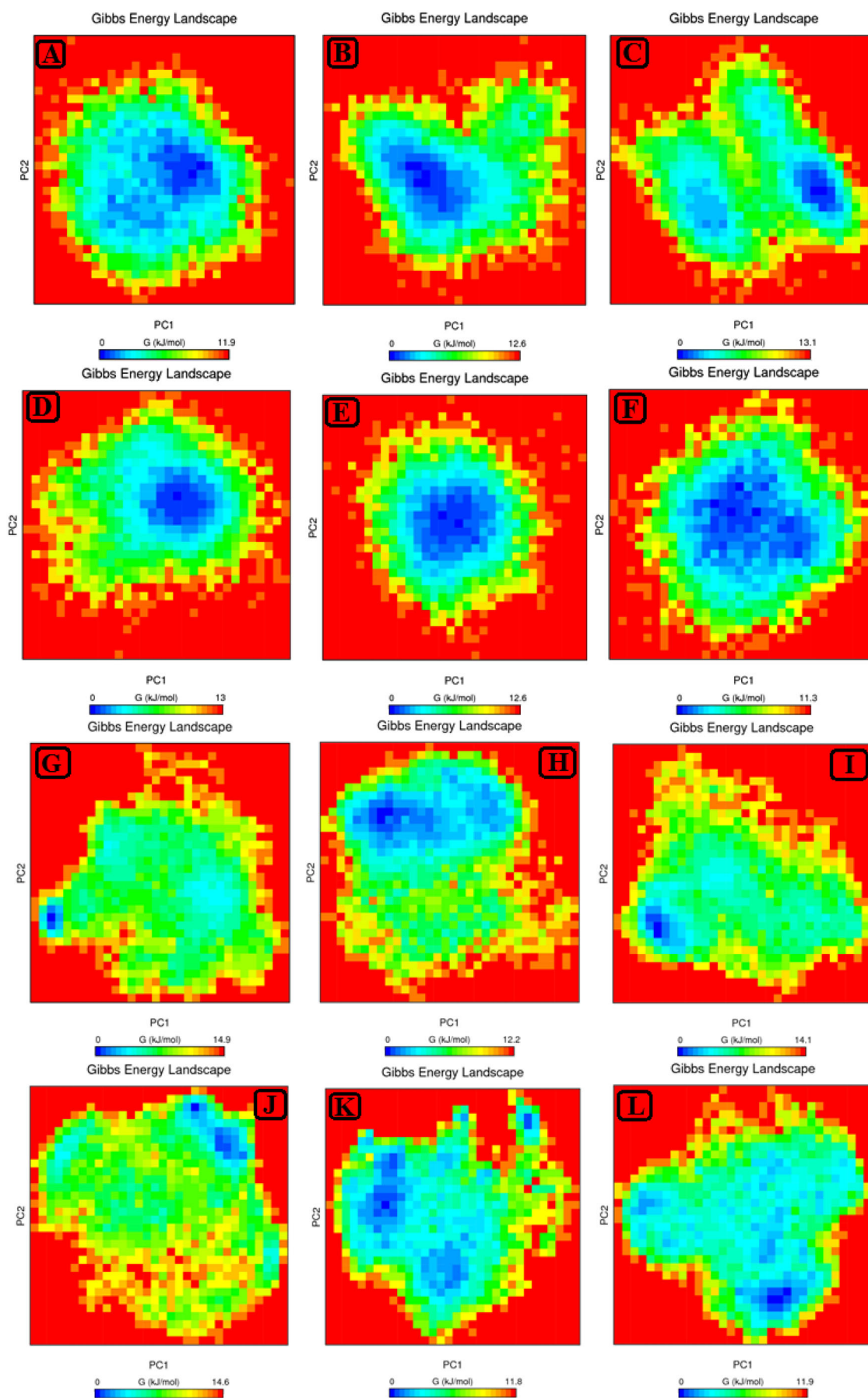
Figure 9. Gibbs free energy landscape: (A–C) Nsp3-Cimetidine, (D–F) Nsp3-Famotidine, (G–I) Nsp7/8-Cimetidine, (J–L) Nsp7/8-Famotidine, (M–O) Nsp9-Cimetidine, and (P–R) Nsp9-Famotidine complexes.
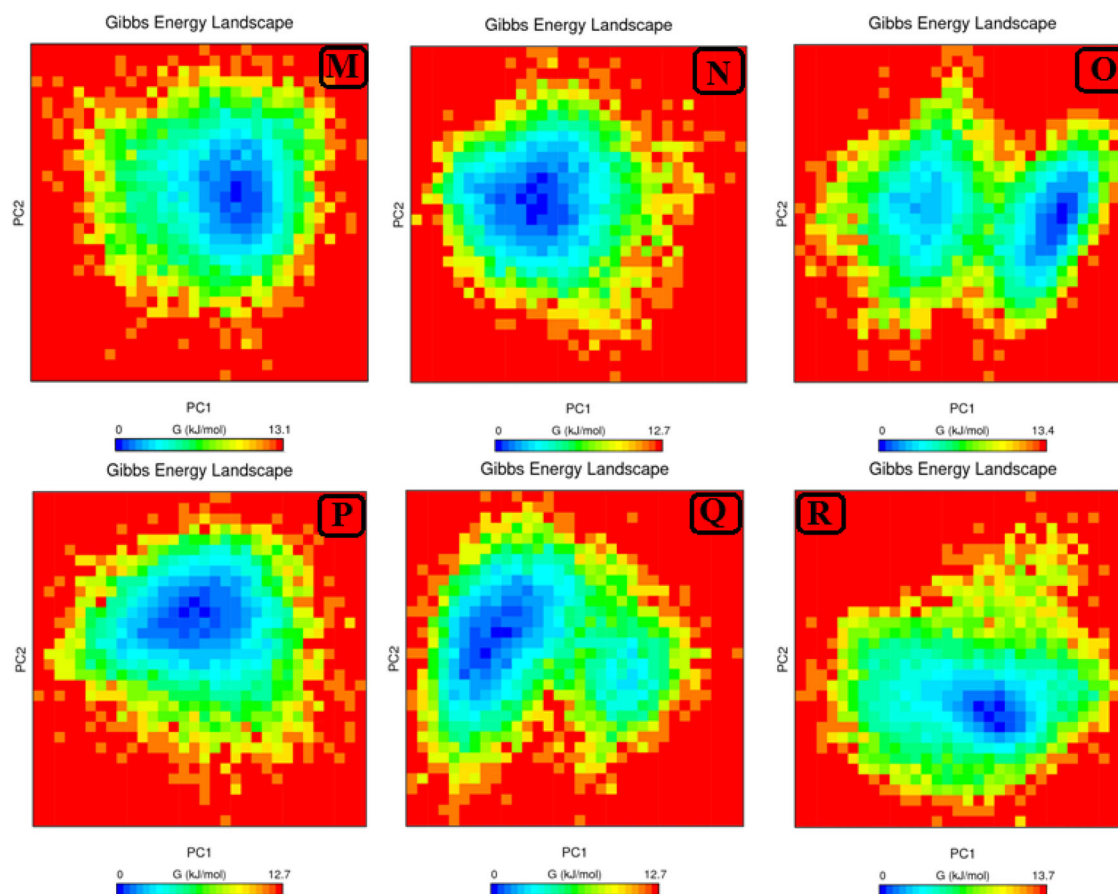
Figure 9. Continued.

Table 5. Table displaying binding energy of Nsp-Famotidine complex obtained by MM–PBSA.

S. no.	Name of Protein-ligand complex	Van der Waal energy	Electrostatic energy	Polar solvation energy	SASA energy	Total energy (kJ mol^{-1})
1	Nsp3-Cimetidine complex	−51.11 +/− 19.49	−9.51 +/− 9.80	37.67 +/− 32.38	−7.84 +/− 2.89	−30.79 +/− 15.35
2	Nsp3-Famotidine complex	−154.07 +/− 0.39	−46.73 +/− 0.63	146.82 +/− 1.82	−16.27 +/− 0.02	−70.30 +/− 1.44
3	Nsp7/8-Cimetidine complex	−20.30 +/− 21.68	−5.42 +/− 9.37	8.43 +/− 35.99	−3.01 +/− 3.23	−20.30 +/− 29.74
4	Nsp7/8-Famotidine complex	−115.73 +/− 0.37	−27.58 +/− 0.36	103.07 +/− 0.62	−13.78 +/− 0.04	−54.03 +/− 0.36
5	Nsp9-Cimetidine complex	−28.64 +/− 26.69	−14.76 +/− 18.30	40.12 +/− 44.68	−4.30 +/− 4.01	−7.58 +/− 25.14
6	Nsp9-Famotidine complex	−83.14 +/− 31.93	−17.49 +/− 15.44	63.22 +/− 33.03	−10.14 +/− 3.27	−47.55 +/− 18.96

Cimetidine complexes and Nsp-Famotidine complexes, considering the last 10 ns of MD trajectories as shown in Table 5. The total binding energies of all the complexes were observed in the acceptable range.

In particular, all Nsp-Famotidine complexes possess the least negative binding energy suggesting a more stable ligand conformation. Nsp3-Famotidine, Nsp7/8-Famotidine, and Nsp9-Cimetidine complexes showed binding energy −70.30 +/− 1.44 kJ mol^{-1}, −54.03 +/− 0.36 kJ mol^{-1}, and −47.55 +/− 18.96 kJ mol^{-1}, respectively. On the other hand, Nsp-Cimetidine complexes displayed −30.79 +/− 15.35 kJ mol^{-1}, −20.30 +/− 29.74 kJ mol^{-1}, and −7.58 +/− 25.14 kJ mol^{-1} free energy for Nsp3-Famotidine, Nsp7/8-Famotidine, and Nsp9-Cimetidine complexes, respectively. It indicates that Famotidine and Cimetidine bind efficiently at the Nsp3, Nsp7/8, and Nsp9's active sites and may be used as a lead molecule to treat COVID-19. Different energy forms of the binding-free energy showed that in all Nsp-Famotidine

complexes evaluated, the leading variable of binding was van der Waals force, which played a significant role in strengthening the binding interactions. Besides, electrostatic energy and SASA non-polar solvation energy contributed similarly to binding energy, although, polar solvation energy did not shown a positive impact on the total binding energy.

The overall MD Simulation (including RMSD, RMSF, and Rg analysis) and Post-MD analysis (including hydrogen bonds, SASA, and PCA) and binding free energy analysis results, we conclude that Famotidine form very stable complexes with Nsp3, Nsp7/8, and Nsp9 and could be effective against COVID-19. However, further researches are required to detect the anti-viral activity of Famotidine.
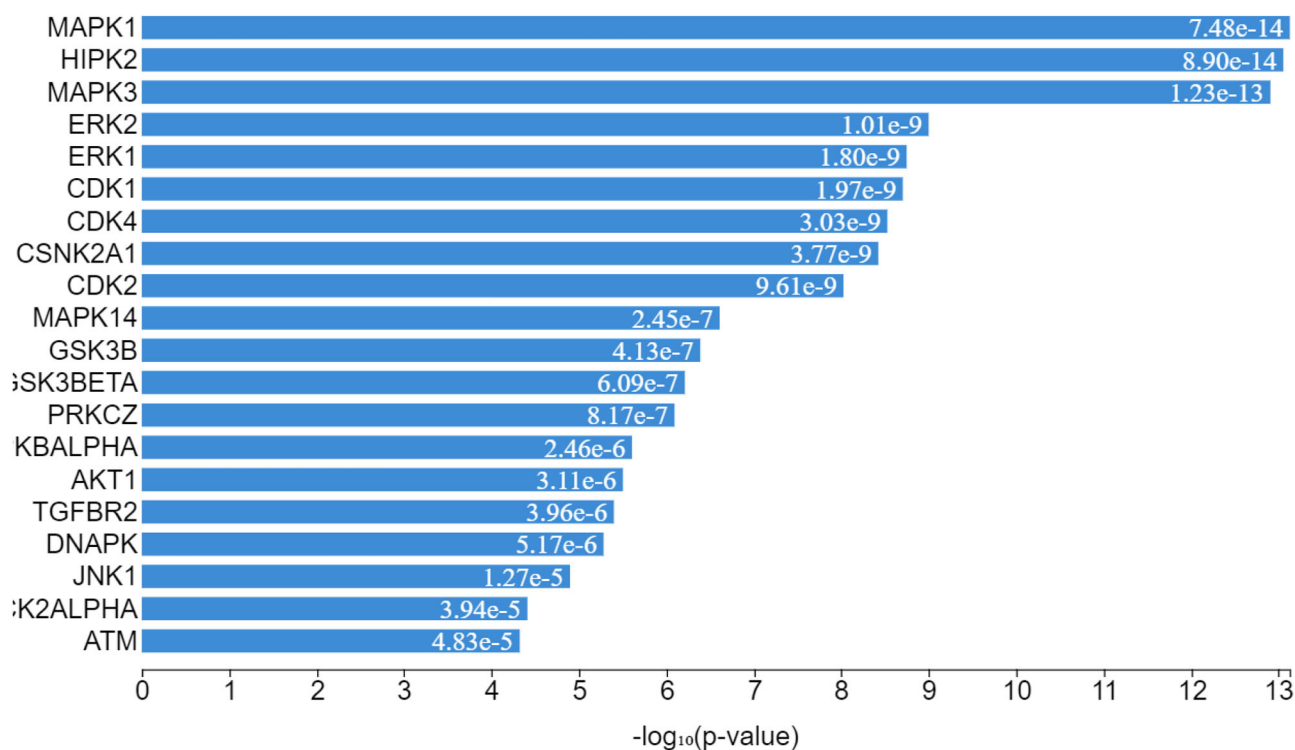
Prediction of target gene

Differential gene expression analysis has become one of the key approaches to identify genes important in the diagnosis

Table 6. Predicted gene targets for Cimetidine and Famotidine.

	Predicted/Known target	Gene code	Precision (%)	Tc
SN	Cytochrome P450 3A5	CYP3A5	72.2	0.625
1	Solute carrier family 22 member 11	SLC22A11	70.6	0.625
2	Solute carrier family 22 member 3	SLC22A3	67.7	0.625
3	Flavin-containing monooxygenase 3	FMO3	63.7	0.625
4	Solute carrier family 22 member 7	SLC22A7	59.1	0.625
5	Multidrug and toxin extrusion protein 1	SLC47A1	58.7	0.625
6	Multidrug and toxin extrusion protein 2	SLC47A2	51.1	0.625
7	Dimethylaniline monooxygenase [N-oxide-forming] 1	FMO1	45.9	0.625
8	Histamine H2 receptor	HRH2	38.7	0.625
9	Histamine H4 receptor	HRH4	29.6	0.625
10	Organic cation transporter 3	OCT3	26.7	0.307
11	Organic anion transporter 3	OAT3	26.3	0.307
12	Cytochrome P450 3A4	CYP3A4	23.8	0.463
13	Cytochrome P450 2D6	CYP2D6	23.3	0.463
14	Cholecystokinin B receptor	CCKBR	26.6	0.324
15	Solute carrier family 22 member 2	SLC22A2	23.4	0.307

Tc = Tanimoto coefficient.

Figure 10. Kinase enrichment analysis for Cimetidine and Famotidine target genes.

and prediction of various diseases. Results from the gene prediction test revealed possible targets such as families of solute carriers (SLC22A11, SLC22A3, SLC22A7, SLC47A1, SLC47A2, SLC22A2), cytochrome p450 (CYP2D6, CYP3A4, CYP3A5), histamine receptors (HRH2, HRH4), and other genes including; Cholecystokinin B receptor (CCKBR), Dimethylaniline monooxygenase [N-oxide-forming] 1 (FMO1) (Table 6). Tanimoto coefficient between the query compound and the closest compound in the k-nearest neighbor (k-NN) chemical space annotated to the predicted target. When Tc = 1 it denotes strong similarity, while Tc = 0 denotes weak similarity. The Tc compares the similarity of Functional-Class Fingerprints (FCFP)-like circular Morgan fingerprints. The precision of the predicted target was calculated within intervals of chemical similarity (Tc), for the first ten ranking predicted targets according to the Bayesian Model scores as well as within target occurrence intervals of the predicted target within such space. Consequently, only five of the predicted targets were above the 50% precision threshold based on the Tanimoto Coefficient. Moreover, the importance of solute carriers (e.g. SLC6A20) in the pathogenesis of the novel coronavirus has been reported (Anastassopoulou et al., 2020). SLC6A20 interacts with the cell-surface receptor of the novel coronavirus, angiotensin-converting enzyme 2 (ACE2) (Kuba et al., 2010; Vuille-Dit-Bille et al., 2015) thereby preventing viral attachment and entry.

Fifteen kinases with the highest hypergeometric p-value found in association with Cimetidine-Famotidine target genes transcription factors include mitogen-activated protein kinases (MAPKs) and cyclin-dependent kinases (CDKs) as shown in Figure 10. These kinases are important in the replication of viruses (Wehbe et al., 2020). Coronaviruses have
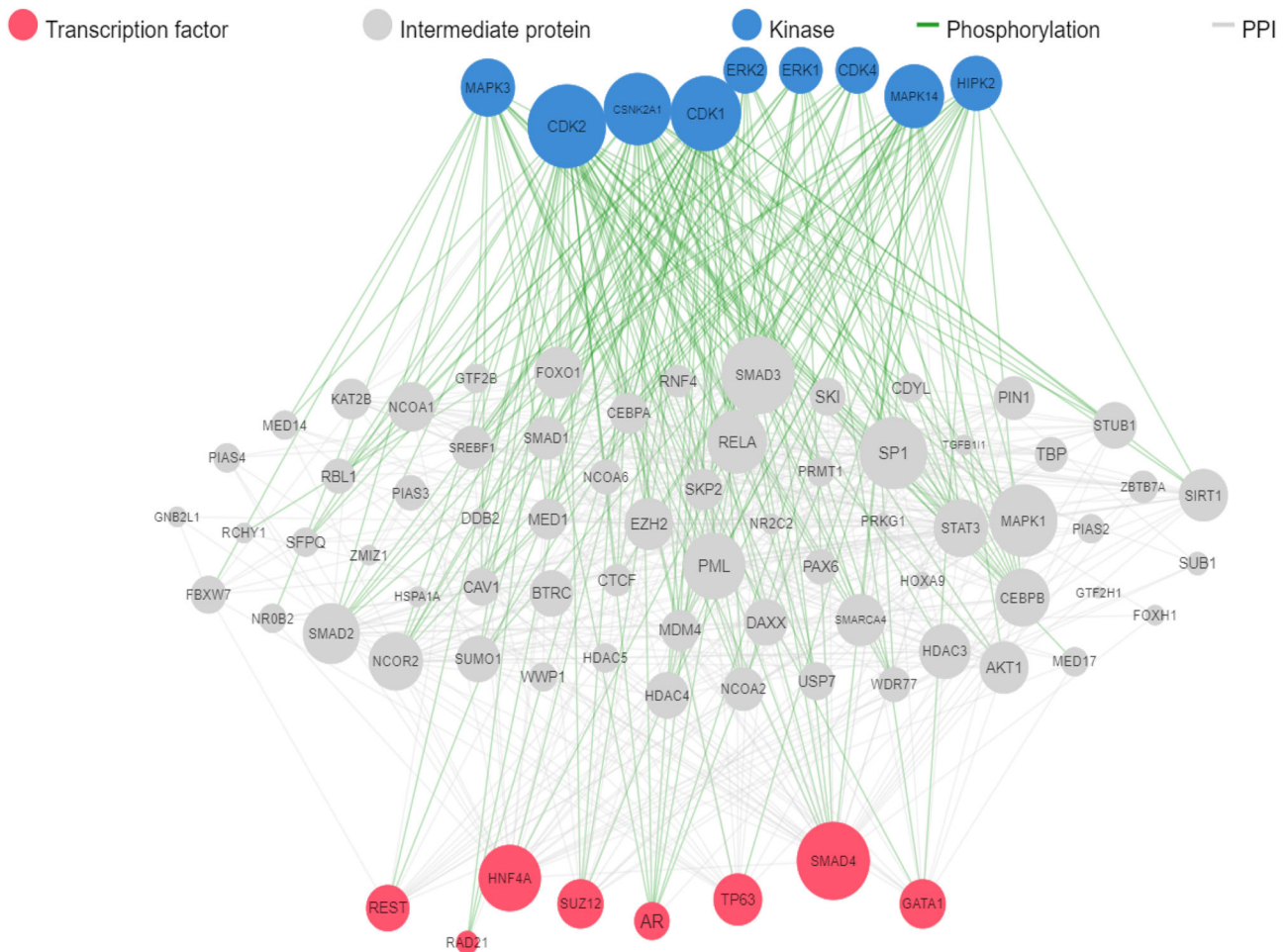
Figure 11. Overall network of genes associated with Cimetidine and Famotidine generated by eXpression2Kinases server.

been reported to involve p38, MAPK, JNK, and MKK1/ERK1/2 pathways for viral pathogenesis. MKK1/ERK1/2 pathway also upregulates the protease furin, which is implicated in SARS-CoV-2 entry due to the unique furin-like S1/S2 cleavage site (Li et al., 2019; Wehbe et al., 2020). Consequently, inhibition of the MEK1/2/ERK1/2 pathway in mice has been reported to significantly impair coronavirus replication by reducing viral progeny (Cai et al., 2007).

The overall network of genes associated with Cimetidine and Famotidine as obtained from the eXpression2Kinases server is shown in Figure 11. The protein-protein interaction showed transcription factors most expressed by Cimetidine/Famotidine-targeted genes based on hypergeometric p-value which include; SMAD family member 4 (SMAD4), RE1-Silencing Transcription factor (REST), Polycomb protein (SUZ12), Hepatocyte nuclear factor 4 alpha (HNF4A), GATA-binding factor 1 (GATA 1), Tumor protein p63 (TP63), these transcription factors have been implicated in the pathogenesis of various biological processes including tumorigenesis, apoptosis, induction chromatin remodeling of the proviral gene, upregulation of genes in response to oxidative stress, regulation of cellular redox conditions, epigenetic repression systems and other molecular functions. The role of SMAD3 in the coronavirus genome has previously been highlighted (Ochsner et al., 2020). SMAD4 is a co-SMAD that binds to receptor-regulated SMADS (R-SMADS) like SMAD1, SMAD2,

SMAD5, and SMAD8 to form heterotrimeric complexes to regulate the expression of different genes (Massagué, 1998) including transforming growth factor-β (TGF-β), a cytokine that pivotal role in pulmonary fibrosis that is common in coronavirus patients (Roberts et al., 2006). The network of genes identified with Cimetidine and Famotidine shows that the compounds were able to interact with genes that are closely related to coronaviruses and can therefore be explored as a treatment of COVID-19 in this moment where the world is threatened by a second wave of COVID-19 pandemic.

Several therapies against the SARS-CoV-2 virus are in the trial to provide a cure for the dreadful viral outbreak of COVID-19. Recently, global attention has turned to preliminary reports on the promising anti-COVID-19 effect of H2RAs. Early data show that H2RAs had antiviral properties inhibiting HIV replication *in vitro* (Bartlett et al., 1998; Bourinbaiar & Fruhstorfer, 1996). Recent research in New York also found that Famotidine use was associated with a decreased risk of intubation or mortality among hospitalized COVID-19 patients (Freedberg et al., 2020). The current study was therefore undertaken to find potent H2RAs which can be used against the SARS-CoV-2 virus using computational techniques. As we are interested in finding potent H2RAs against SARS-CoV-2, therefore, this study was designed to identify the possible molecular mechanism for the anti-viral efficacy of four H2RAs viz. Famotidine, Nizatidine, Cimetidine, and

Ranitidine against SARS-CoV-2. All compounds possessed good pharmacokinetic properties. Also, all compounds exhibited reasonable broad antiviral activities, such as Cimetidine, Nizatidine, and Ranitidine, demonstrating better inhibitory activity of Human Immunodeficiency Virus (HIV), while Famotidine demonstrated better inhibitory activity toward Hepatitis C Virus (HCV) and Human herpes virus (HCV). The molecular docking was performed between four H2RAs Cimetidine, Famotidine, Nizatidine, and Ranitidine with three SARS-CoV-2 non-structural proteins viz. NSP3, NSP7/8 complex, and NSP9, which indicates the superiority of Famotidine and Cimetidine compared with other H2RAs. It effectively docked against the SARS-CoV-2 non-structural protein's inhibitor region and showed a high potential for binding to the selected targets. Famotidine and Cimetidine possesses excellent pharmacokinetic properties of drug ability, small molecular weight and, molar refractivity which confirms that it is permeable through particular membranes and can remain constant even in strong or weak solute-solvent, solvent-solvent interactions. Drug-likeness RO5 was obeyed by Famotidine which describes that it can act as a drug in the biological systems. The toxicity prediction says that Famotidine and Cimetidine are safe and can be given as a drug with the value of tolerance prescribed for human consumption as predicted by OSIRIS. Finally, a 100 ns MD simulation verified the relative stability of Cimetidine-NSPs and Famotidine-NSPs complexes. The MD trajectories analysis indicates that Famotidine and Cimetidine bind to the SARS-CoV-2 NSPs efficiently and displayed structural stability during the simulation period. Binding free energy analysis by MMPBSA shows of Famotidine shows the excellent binding energy toward all NSPs. Results obtained suggest that histamine H2-receptor antagonist; Famotidine and Cimetidine are potent inhibitors of SARS-CoV-2 and could be a viable treatment option for COVID-19. This study may be helpful to develop effective medications against COVID-19 in the future.

Conclusion

The current study aimed to identify novel potent H2RAs against the SARS-CoV-2 non-structural proteins. For this purpose, we employed various computational methods like molecular docking, Molecular Dynamics Simulation, MM-PBSA analysis and gene prediction analysis. Here, we used four H2RAs viz. Famotidine, Nizatidine, Cimetidine, and Ranitidine for molecular docking against three SARS-CoV-2 non-structural proteins viz. NSP3, NSP7/8 complex, and NSP9. Based on molecular docking, and binding affinity Famotidine and Cimetidine were selected as lead compounds against SARS-CoV-2 NSPs. From the MD simulation and binding free energy results, we concluded that Famotidine and Cimetidine are the stable compounds that showed excellent binding affinities with all NSPs during 100 ns simulation. Gene prediction analysis of Famotidine and Cimetidine identified important transcription factors and genes such as MAPKs, ERKs and SMADs that play crucial roles in the pathogenesis of COVID-19. Thus, this study's outcome shows that the antiviral potential of Famotidine and Cimetidine could

pose a great deal of significance against COVID-19. This *in silico* study suggested that Famotidine and Cimetidine may be explored as a novel lead molecule for the rapid development of suitable drug candidates against COVID-19.

ORCID

Habibu Tijjani 🆔 http://orcid.org/0000-0001-5466-322X
Subhash Chandra 🆔 http://orcid.org/0000-0002-8978-5427

References

Adachi, K., Komazawa, Y., Mihara, T., Azumi, T., Fujisawa, T., Katsube, T., Furuta, K., & Kinoshita, Y. (2005). Comparative study of the speed of acid-suppressing effects of oral administration of cimetidine and famotidine. *Journal of Gastroenterology and Hepatology*, *20*(7), 1012–1015. https://doi.org/10.1111/j.1440-1746.2005.03917.x

Anastassopoulou, C., Gkizarioti, Z., Patrinos, G. P., & Tsakris, A. (2020). Human genetic factors associated with susceptibility to SARS-CoV-2 infection and COVID-19 disease severity. *Human Genomics*, *14*(1), 1–8. https://doi.org/10.1186/s40246-020-00290-4

Bartlett, J. A., Berry, P. S., Bockman, K. W., Stein, A., Johnson, J., Graham, S., Quinn, J., DeMasi, R., & Alexander, W. J. (1998). A placebo-controlled trial of ranitidine in patients with early human immunodeficiency virus infection. *The Journal of Infectious Diseases*, *177*(1), 231–234. https://doi.org/10.1086/517361

Bourinbaiar, A. S., & Fruhstorfer, E. C. (1996). The effect of histamine type 2 receptor antagonists on human immunodeficiency virus (HIV) replication: Identification of a new class of antiviral agents. *Life Sciences*, *59*(23), PL365–PL370. https://doi.org/10.1016/S0024-3205(96)00553-X

Cai, Y., Liu, Y., & Zhang, X. (2007). Suppression of coronavirus replication by inhibition of the MEK signaling pathway. *Journal of Virology*, *81*(2), 446–456. https://doi.org/10.1128/JVI.01705-06

Clarke, D. J. B., Kuleshov, M. V., Schilder, B. M., Torre, D., Duffy, M. E., Keenan, A. B., Lachmann, A., Feldmann, A. S., Gundersen, G. W., Silverstein, M. C., Wang, Z., & Ma'ayan, A. (2018). EXpression2Kinases (X2K) Web: Linking expression signatures to upstream cell signaling networks. *Nucleic Acids Research*, *46*(W1), W171–W179. https://doi.org/10.1093/nar/gky458

Dassault, S. (2020). BIOVIA, Discovery Studio Visualizer, 2020. Discovery Studio Client. https://discover.3ds.com/discovery-studio-visualizer-download

Forni, D., Cagliani, R., Mozzi, A., Pozzoli, U., Al-Daghri, N., Clerici, M., & Sironi, M. (2016). Extensive positive selection drives the evolution of nonstructural proteins in lineage C betacoronaviruses. *Journal of Virology*, *90*(7), 3627–3639. https://doi.org/10.1128/JVI.02988-15

Freedberg, D. E., Conigliaro, J., Wang, T. C., Tracey, K. J., Callahan, M. V., Abrams, J. A., Sobieszczyk, M. E., Markowitz, D. D., Gupta, A.,

O'Donnell, M. R., Li, J., Tuveson, D. A., Jin, Z., Turner, W. C., & Landry, D. W. (2020). Famotidine use is associated with improved clinical outcomes in hospitalized COVID-19 patients: A propensity score matched retrospective cohort study. *Gastroenterology*, 159(3), 1129–1131.e3. https://doi.org/10.1053/j.gastro.2020.05.053

Goodsell, D. S., Morris, G. M., & Olson, A. J. (1996). Automated docking of flexible ligands: Applications of AutoDock. *Journal of Molecular Recognition*, 9(1), 1–5. https://doi.org/10.1002/(SICI)1099-1352(199601)9:1<1::AID-JMR241>3.0.CO;2-6

Hamad, S., Adornetto, G., Naveja, J. J., Chavan Ravindranath, A., Raffler, J., & Campillos, M. (2019). HitPickV2: A web server to predict targets of chemical compounds. *Bioinformatics (Oxford, England)*, 35(7), 1239–1240. https://doi.org/10.1093/bioinformatics/bty759

Ishola, A. A., & Asogwa, N. T. (2020). Homology modeling of coronavirus structural proteins and molecular docking of potential drug candidates for the treatment of COVID-19. *Coronaviruses*, 01 (2), 1-10 . https://doi.org/10.2174/2666796701999200802040704

Izadi, S., & Onufriev, A. V. (2016). Accuracy limit of rigid 3-point water models. *The Journal of Chemical Physics*, 145(7), 074501. https://doi.org/10.1063/1.4960175

Jafarzadeh, A., Nemati, M., Khorramdelazad, H., & Hassan, Z. M. (2019). Immunomodulatory properties of cimetidine: Its therapeutic potentials for treatment of immune-related diseases. *International Immunopharmacology*, 70, 156–166. https://doi.org/10.1016/j.intimp.2019.02.026

Janowitz, T., Gablenz, E., Pattinson, D., Wang, T. C., Conigliaro, J., Tracey, K., & Tuveson, D. (2020). Famotidine use and quantitative symptom tracking for COVID-19 in non-hospitalised patients: A case series. *Gut*, 69(9), 1592–1597. https://doi.org/10.1136/gutjnl-2020-321852

Ji, W., Wang, W., Zhao, X., Zai, J., & Li, X. (2020). Homologous recombination within the spike glycoprotein of the newly identified coronavirus may boost cross-species transmission from snake to human. *Journal of Medical Virology*, 92(4), 433–440. https://doi.org/10.1002/jmv.25682

Kuba, K., Imai, Y., Ohto-Nakanishi, T., & Penninger, J. M. (2010). Trilogy of ACE2: A peptidase in the renin-angiotensin system, a SARS receptor, and a partner for amino acid transporters. *Pharmacology & Therapeutics*, 128(1), 119–128. https://doi.org/10.1016/j.pharmthera.2010.06.003

Kumari, R., Kumar, R., Consortium, O. S. D. D., Lynn, A, & Open Source Drug Discovery Consortium. (2014). g_mmpbsa-a GROMACS tool for high-throughput MM-PBSA calculations. *Journal of Chemical Information and Modeling*, 54(7), 1951–1962. https://doi.org/10.1021/ci500020m

Lei, J., Kusov, Y., & Hilgenfeld, R. (2018). Nsp3 of coronaviruses: Structures and functions of a large multi-domain protein. *Antiviral Research*, 149, 58–74. https://doi.org/10.1016/j.antiviral.2017.11.001

Li, C. C., Wang, X. J., & Wang, H. C. R. (2019). Repurposing host-based therapeutics to control coronavirus and influenza virus. *Drug Discovery Today*, 24(3), 726–736. https://doi.org/10.1016/j.drudis.2019.01.018

Littler, D. R., Gully, B. S., Colson, R. N., & Rossjohn, J. (2020). Crystal structure of the SARS-CoV-2 non-structural protein 9, Nsp9. *iScience*, 23(7), 101258. https://doi.org/10.1016/j.isci.2020.101258

Massagué, J. (1998). TGF-beta signal transduction. *Annual Review of Biochemistry*, 67, 753–791. https://doi.org/10.1146/annurev.biochem.67.1.753

Michalska, K., Kim, Y., Jedrzejczak, R., Maltseva, N., Stols, L., Endres, M., & Joachimiak, A. (2020). Crystal structures of SARS-CoV-2 ADP-ribose phosphatase (ADRP): From the apo form to ligand complexes. *IUCrJ*, 7(5), 814–824. https://doi.org/10.1101/2020.05.14.096081

O'Boyle, N. M., Banck, M., James, C. A., Morley, C., Vandermeersch, T., & Hutchison, G. R. (2011). Open Babel: An open chemical toolbox. *Journal of Cheminformatics*, 3(10), 33. https://doi.org/10.1186/1758-2946-3-33

Ochsner, S. A., Pillich, R. T., & McKenna, N. J. (2020). Consensus transcriptional regulatory networks of coronavirus-infected human cells. *Scientific Data*, 7(1), 1–20. https://doi.org/10.1038/s41597-020-00628-6

Peng, Q., Peng, R., Yuan, B., Zhao, J., Wang, M., Wang, X., Wang, Q., Sun, Y., Fan, Z., Qi, J., Gao, G. F., & Shi, Y. (2020). Structural and biochemical characterization of the nsp12-nsp7-nsp8 core polymerase complex from SARS-CoV-2. *Cell Reports*, 31(11), 107774. https://doi.org/10.1016/j.celrep.2020.107774

Pronk, S., Páll, S., Schulz, R., Larsson, P., Bjelkmar, P., Apostolov, R., Shirts, M. R., Smith, J. C., Kasson, P. M., Van Der Spoel, D., Hess, B., & Lindahl, E. (2013). GROMACS 4.5: A high-throughput and highly parallel open source molecular simulation toolkit. *Bioinformatics (Oxford, England)*, 29(7), 845–854. https://doi.org/10.1093/bioinformatics/btt055

Qureshi, A., Kaur, G., & Kumar, M. (2017). AVCpred: An integrated web server for prediction and design of antiviral compounds. *Chemical Biology & Drug Design*, 89(1), 74–83. https://doi.org/10.1111/cbdd.12834

Roberts, A. B., Tian, F., Byfield, S. D. C., Stuelten, C., Ooshima, A., Saika, S., & Flanders, K. C. (2006). Smad3 is key to TGF-beta-mediated epithelial-to-mesenchymal transition, fibrosis, tumor suppression and metastasis. *Cytokine & Growth Factor Reviews*, 17(1–2), 19–27. https://doi.org/10.1016/j.cytogfr.2005.09.008

Sánchez-Linares, I., Pérez-Sánchez, H., Cecilia, J. M., & García, J. M. (2012). High-throughput parallel blind virtual screening using BINDSURF. *BMC Bioinformatics*, 13(Suppl 14), S13. https://doi.org/10.1186/1471-2105-13-S14-S13

Sutton, G., Fry, E., Carter, L., Sainsbury, S., Walter, T., Nettleship, J., Berrow, N., Owens, R., Gilbert, R., Davidson, A., Siddell, S., Poon, L. L. M., Diprose, J., Alderton, D., Walsh, M., Grimes, J. M., & Stuart, D. I. (2004). The nsp9 replicase protein of SARS-coronavirus, structure and functional insights. *Structure (London, England: 1993)*, 12(2), 341–353. https://doi.org/10.1016/j.str.2004.01.016

Trott, O., & Olson, A. J. (2010). AutoDock Vina: Improving the speed and accuracy of docking with a new scoring function, efficient optimization, and multithreading. *Journal of Computational Chemistry*, 31(2), 455–461. https://doi.org/10.1002/jcc.21334

Vanommeslaeghe, K., Hatcher, E., Acharya, C., Kundu, S., Zhong, S., Shim, J., Darian, E., Guvench, O., Lopes, P., Vorobyov, I., & Mackerell, A. D., Jr. (2009). CHARMM general force field: A force field for drug-like molecules compatible with the CHARMM all-atom additive biological force fields. *Journal of Computational Chemistry*, 31(4), 671–690.

Vuille-Dit-Bille, R. N., Camargo, S. M., Emmenegger, L., Sasse, T., Kummer, E., Jando, J., Hamie, Q. M., Meier, C. F., Hunziker, S., Forras-Kaufmann, Z., Kuyumcu, S., Fox, M., Schwizer, W., Fried, M., Lindenmeyer, M., Götze, O., & Verrey, F. (2015). Human intestine luminal ACE2 and amino acid transporter expression increased by ACE-inhibitors. *Amino Acids*, 47(4), 693–705. https://doi.org/10.1007/s00726-014-1889-6

Wehbe, Z., Hammoud, S., Soudani, N., Zaraket, H., El-Yazbi, A., & Eid, A. H. (2020). Molecular insights into SARS COV-2 interaction with cardiovascular disease: Role of RAAS and MAPK signaling. *Frontiers in Pharmacology*, 11, 836. https://doi.org/10.3389/fphar.2020.00836

WHO. (2020). *Coronavirus disease (COVID-2019) situation reports*, 168. https://www.who.int/docs/default-source/coronaviruse/situation-reports/20200706-covid-19-sitrep-168.pdf?sfvrsn=7fed5c0b_2

Wilamowski, M., Kim, Y., Jedrzejczak, R., Maltseva, N., Endres, M., Godzik, A., Michalska, K., Joachimiak, A. (2020). Crystal structure of the co-factor complex of NSP7 and the C-terminal domain of NSP8 from SARS CoV-2. https://www.ncbi.nlm.nih.gov/Structure/pdb/

Yoshimoto, F. K. (2020). The proteins of severe acute respiratory syndrome coronavirus-2 (SARS CoV-2 or n-COV19), the cause of COVID-19. *The Protein Journal*, 39(3), 198–216. https://doi.org/10.1007/s10930-020-09901-4